FERMILAB-PUB-08-046-E

Observation of anomalous multi-muon events produced in $p\bar{p}$ interactions at $\sqrt{s} = 1.96$ TeV

(CDF collaboration)

Abstract

We report the observation of anomalous multi-muon events produced at the Fermilab Tevatron collider and recorded by the CDF II detector. In a data set acquired with a dedicated dimuon trigger and corresponding to an integrated luminosity of 2100 pb^{-1}, we isolate a large sample of events in which at least one of the identified muons is produced outside of the beam pipe of radius 1.5 cm. The production cross section and kinematics of events in which both muons are produced inside the beam pipe are successfully modeled by known standard model (SM) processes which include heavy flavor production. In contrast, we are presently unable to fully account for the size and properties of the remaining events in terms of known SM processes in conjunction with our understanding of the CDF II detector, trigger, and event reconstruction. We show that these events offer a plausible resolution to long-standing inconsistencies related to $b\bar{b}$ production and decay. In a fraction of these events, the muon impact parameter distribution is completely different from that of SM processes and the muon multiplicity is also anomalously large. The topological and kinematic properties of the anomalous events are discussed in the paper.

PACS numbers: 13.85.-t, 14.65.Fy, 14.60.Fg, 14.80.-j, 12.80.Cp, 12.60.Fr, 12.60.Jr

I. INTRODUCTION

This article presents the observation of events, acquired with a dedicated dimuon trigger, with rather striking characteristics that cannot be explained by known SM processes in conjunction with our current understanding of the CDF II detector, trigger, and event reconstruction. We are continuing detailed studies with a longer time for completion, but we present here our current findings because of the possible importance of this observation.

This study was motivated by the presence of several inconsistencies that affect or affected the $b\bar{b}$ production at the Tevatron: (a) the ratio of the observed $b\bar{b}$ correlated production cross section to the exact next-to-leading-order (NLO) QCD prediction [1] is 1.15 ± 0.21 when b quarks are selected via secondary vertex identifications, whereas this ratio is found to be significantly larger than two when identifying b quarks through their semileptonic decays [2]; (b) sequential semileptonic decays of single b quarks are supposedly the main source of dileptons with invariant mass smaller than that of b quarks, but the observed invariant mass spectrum is not well modeled by the SM simulation of this process [3]; and (c) the value of $\bar{\chi}$, the average time integrated mixing probability of b flavored hadrons derived from the ratio of muon pairs from semileptonic decays of b and $\bar{b}$ quarks with opposite and same sign charge, is measured at hadron colliders to be larger than that measured by the LEP experiments [4, 5].

In a recent study [6], the CDF collaboration has used a data sample acquired with a dedicated dimuon trigger to re-measure the correlated $\sigma_{b\to\mu,\bar{b}\to\mu}$ cross section. As in previous studies [4, 7], Ref. [6] makes use of the precision tracking provided by the CDF silicon microvertex detector to evaluate the fractions of muons due to long-lived b- and c-hadron decays, and to the other background contributions. The new measurement is in good agreement with theoretical expectations as well as with analogous measurements that identify b quarks via secondary vertex identification. However, it is also substantially smaller than previous measurements of this cross section [7, 8].

The present study starts with investigating whether the discrepancy with previous measurements is the result of experimental difficulties. The new CDF measurement requires that both trigger muons arise from particles that have decayed inside the beam pipe of 1.5 cm radius. According to the simulation, approximately 96% of the known SM sources of dimuons, such as Drell-Yan, Υ, Z^0, and heavy flavor production, satisfy this condition.

We will show that not only the size, but also the kinematic properties of the events that satisfy this condition are correctly modeled by a SM simulation. However, this article also presents the observation of a much larger than expected component that does not satisfy this condition. This component, which was an issue in previous measurements in which this requirement was not made, will be described and investigated at length in this article. The investigation reveals the presence of a class of anomalous events, of which we anticipate some characteristics here. The muon impact parameter [1] distribution corresponds to a lifetime different from that of known particles. A significant fraction of the distribution extends several times beyond the point where the $b\bar{b}$ contribution has been exhausted. In small angular cones around the direction of the trigger muons, the rate of additional muons and tracks is anomalously high compared to that expected from known SM sources. The invariant mass between trigger and additional muons does not look like that expected from sequential semileptonic B decays. The extent and details of these observations will become apparent in the following sections, in addition to several other interesting characteristics of these anomalous events.

We utilize the same dimuon data set, the same simulated samples, and same analysis tools described in Ref. [6]. Section II describes the detector systems relevant to this analysis. The data selection and Monte Carlo simulation are briefly summarized in Sec. III. Section IV investigates differences in the experimental methods used to derive $\sigma_{b\to\mu,\bar{b}\to\mu}$ in Ref. [6] and in previous measurements, and isolates the presence of an unexpected background with features that may be able to explain this discrepancy as well as the $\bar{\chi}$ puzzle. Section V connects the presence of this background to the anomaly in the observed invariant mass spectrum of lepton pairs produced by single b quark sequential decays. The properties of this unexpected background are explored in Secs. VI and VII. Our conclusions are summarized in Sec. VIII.

II. CDF II DETECTOR AND TRIGGER

CDF II is a multipurpose detector, equipped with a charged particle spectrometer and a finely segmented calorimeter. In this section, we describe the detector components that are relevant to this analysis. The description of these subsystems can be found in Refs. [9–18].

[1] The impact parameter d is the distance of closest approach of a track to the primary event vertex in the transverse plane.

Two devices inside the 1.4 T solenoid are used for measuring the momentum of charged particles: the silicon vertex detector (SVXII and ISL) and the central tracking chamber (COT). The SVXII detector consists of microstrip sensors arranged in six cylindrical shells with radii between 1.5 and 10.6 cm, and with a total z coverage [2] of 90 cm. The first SVXII layer, also referred to as the L00 detector, is made of single-sided sensors mounted on the beryllium beam pipe. The remaining five SVXII layers are made of double-sided sensors and are divided into three contiguous five-layer sections along the beam direction z. The vertex z-distribution for $p\bar{p}$ collisions is approximately described by a Gaussian function with a sigma of 28 cm. The transverse profile of the Tevatron beam is circular and has an rms spread of $\simeq 25$ μm in the horizontal and vertical directions. The SVXII single-hit resolution is approximately 11 μm and allows a track impact parameter resolution of approximately 35 μm, when also including the effect of the beam transverse size. The two additional silicon layers of the ISL help to link tracks in the COT to hits in the SVXII. The COT is a cylindrical drift chamber containing 96 sense wire layers grouped into eight alternating superlayers of axial and stereo wires. Its active volume covers $|z| \leq 155$ cm and 40 to 140 cm in radius. The transverse momentum resolution of tracks reconstructed using COT hits is $\sigma(p_T)/p_T^2 \simeq 0.0017$ $[\mathrm{GeV}/c]^{-1}$. COT tracks are extrapolated into the SVXII detector and refitted adding hits consistent with the track extrapolation.

The central muon detector (CMU) is located around the central electromagnetic and hadronic calorimeters, which have a thickness of 5.5 interaction lengths at normal incidence. The CMU detector covers a nominal pseudorapidity range $|\eta| \leq 0.63$ relative to the center of the detector, and is segmented into two barrels of 24 modules, each covering 15° in ϕ. Every module is further segmented into three submodules, each covering 4.2° in ϕ and consisting of four layers of drift chambers. The smallest drift unit, called a stack, covers a 1.2° angle in ϕ. Adjacent pairs of stacks are combined together into a tower. A track segment (hits in two out of four layers of a stack) detected in a tower is referred to as a CMU stub. A second set of muon drift chambers (CMP) is located behind an additional

[2] In the CDF coordinate system, θ and ϕ are the polar and azimuthal angles of a track, respectively, defined with respect to the proton beam direction, z. The pseudorapidity η is defined as $-\ln\ \tan(\theta/2)$. The transverse momentum of a particle is $p_T = p\ \sin(\theta)$. The rapidity is defined as $y = 1/2 \cdot \ln((E + p_z)/(E - p_z))$, where E and p_z are the energy and longitudinal momentum of the particle associated with the track.

steel absorber of 3.3 interaction lengths. The chambers are 640 cm long and are arranged axially to form a box around the central detector. The CMP detector covers a nominal pseudorapidity range $|\eta| \leq 0.54$ relative to the center of the detector. Muons which produce a stub in both the CMU and CMP systems are called CMUP muons. The CMX muon detector consists of eight drift chamber layers and scintillation counters positioned behind the hadron calorimeter. The CMX detector extends the muon coverage to $|\eta| \leq 1$ relative to the center of the detector.

The luminosity is measured using gaseous Cherenkov counters (CLC) that monitor the rate of inelastic $p\bar{p}$ collisions. The inelastic $p\bar{p}$ cross section at $\sqrt{s} = 1960$ GeV is scaled from measurements at $\sqrt{s} = 1800$ GeV using the calculations in Ref. [19]. The integrated luminosity is determined with a 6% systematic uncertainty [20].

CDF uses a three-level trigger system. At Level 1 (L1), data from every beam crossing are stored in a pipeline capable of buffering data from 42 beam crossings. The L1 trigger either rejects events or copies them into one of the four Level 2 (L2) buffers. Events that pass the L1 and L2 selection criteria are sent to the Level 3 (L3) trigger, a cluster of computers running speed-optimized reconstruction code.

For this study, we select events with two muon candidates identified by the L1 and L2 triggers. The L1 trigger uses tracks with $p_T \geq 1.5$ GeV/c found by a fast track processor (XFT). The XFT examines COT hits from the four axial superlayers and provides $r - \phi$ information. The XFT finds tracks with $p_T \geq 1.5$ GeV/c in azimuthal sections of 1.25°. The XFT passes the tracks to a set of extrapolation units that determine the CMU towers in which a CMU stub should be found if the track is a muon. If a stub is found, a L1 CMU primitive is generated. The L1 dimuon trigger requires at least two CMU primitives, separated by at least two CMU towers. The L2 trigger additionally requires that at least one of the muons has a CMUP stub matched to an XFT track with $p_T \geq 3$ GeV/c. All these trigger requirements are emulated by the detector simulation on a run-by-run basis. The L3 trigger requires a pair of CMUP muons with invariant mass larger than 5 GeV/c^2, and $|\delta z_0| \leq 5$ cm, where z_0 is the z coordinate of the muon track at its point of closest approach to the beam line in the $r - \phi$ plane. These requirements define the dimuon trigger used in this analysis.

We also use events acquired requiring a L1 CMUP primitive with $p_T \geq 4$ GeV/c accompanied by a L2 requirement of an additional track with $p_T \geq 2$ GeV/c and impact parameter

$0.12 \leq d \leq 1$ mm as measured by the Silicon Vertex Trigger (SVT) [21]. The SVT calculates the impact parameter of each XFT track, with respect to the beam line, with a 50 μm resolution that includes the 25 μm contribution of the beam transverse width. Events selected with this trigger, referred to as $\mu-$SVT, are used to verify the muon detector acceptance and the muon reconstruction efficiency. We use an additional trigger, referred to as CHARM, that acquires events with two SVT tracks with $p_T \geq 2$ GeV/c and with impact parameter $0.12 \leq d \leq 1$ mm. In this data sample, we reconstruct $D^0 \rightarrow K\pi$ decays to measure the probability that a charged hadron mimics a muon signal.

III. DATA SELECTION AND MONTE CARLO SIMULATIONS

This study uses the same data set and analysis selection criteria employed in the measurement of the correlated $b\bar{b}$ cross section [6], but also takes advantage of all available integrated luminosity. The correlated $b\bar{b}$ cross section measurement selects events acquired with the dimuon trigger and which contain at least two CMUP muons with same or opposite sign charge. If events contain more than two muons that pass our selection cuts, the two with the highest transverse momenta, referred to as initial muons, are considered. Events are reconstructed offline taking advantage of more refined calibration constants and reconstruction algorithms. COT tracks are extrapolated into the SVXII detector, and refitted adding hits consistent with the track extrapolation. Stubs reconstructed in the CMU and CMP detectors are matched to tracks with $p_T \geq 3$ GeV/c. A track is identified as a CMUP muon if $\Delta r\phi$, the distance in the $r-\phi$ plane between the track projected to the CMU (CMP) chambers and a CMU (CMP) stub, is less than 20 (40) cm. We require that muon-candidate stubs correspond to a L1 CMU primitive, and correct the muon momentum for energy losses in the detector. We also require that the z_0 distance between two muon candidates be less than 1.5 cm. We reconstruct primary vertices using all tracks with SVXII hits that are consistent with originating from a common vertex. In events in which more than one interaction vertex has been reconstructed we use the one closest in z to the average of the muon track z_0-positions and within a 6 cm distance. We evaluate the impact parameter of each muon track with respect to the primary vertex. Events contributed by cosmic rays are removed by requiring that the azimuthal angle between muons with opposite charge is smaller than 3.135 radians. Muon pairs arising from cascade decays of a single b quark are removed by

selecting dimuon candidates with invariant mass greater than 5 GeV/c^2. We also reject muon pairs with invariant mass larger than 80 GeV/c^2 that are mostly contributed by Z^0 decays. These selection criteria reduce the size of the data sample to 743006 events.

In this study, data are compared to different simulated samples. The heavy flavor production is simulated with the HERWIG Monte Carlo program [22], the settings of which are described in Appendix A of Ref. [6]. Hadrons with heavy flavors are subsequently decayed using the EVTGEN Monte Carlo program [23]. The detector response to particles produced by the above generators is modeled with the CDF II detector simulation that in turn is based on the GEANT Monte Carlo program [24].

IV. STUDY OF THE DATA SAMPLE COMPOSITION

The procedure to extract $\sigma_{b\to\mu,\bar{b}\to\mu}$ from the data is to fit the observed impact parameter distributions of the selected dimuons with the expected impact parameter distributions of muons from various sources. To ensure an accurate impact parameter measurement, Ref. [6] requires that each muon track is reconstructed in the SVXII detector with hits in the two inner layers and in at least two of the remaining four external layers. These SVXII quality requirements reduce the data sample to 143743 events. After this selection, the known sources of reconstructed muons are semileptonic decays of bottom and charmed hadrons, prompt decays of quarkonia, Drell-Yan production, and muons mimicked by prompt hadrons or hadrons arising from heavy flavor decays. In the following, the sum of these contributions will be often referred to as QCD production. Monte Carlo simulations are used to model the impact parameter distributions of muons from b- and c-hadron decays. The impact parameter distribution of muons from prompt sources, such as quarkonia decays and Drell-Yan production, is constructed using muons from $\Upsilon(1S)$ decays. The sample composition determined by the fit is shown in Table I. After removing the contribution of muons mimicked by hadrons from heavy flavor decays, the study in Ref. [6] determines the size of $b\bar{b}$ production to be 52400 ± 2747 events. For muons with $p_T \geq 3$ GeV/c and $|\eta| \leq 0.7$, Ref. [6] reports $\sigma_{b\to\mu,\bar{b}\to\mu} = 1549 \pm 133$ pb. The ratio of this cross section to the NLO prediction (1.20 ± 0.21) is appreciably smaller than that reported by previous experiments [7, 8], and in agreement with the correlated $b\bar{b}$ cross section measurements that select b quarks via secondary vertex identification (1.15 ± 0.21) [26, 27]. This result mitigates

TABLE I: Number of events attributed to the different dimuon sources by the fit to the muon impact-parameter distribution in the range $0 - 0.2$ cm. The fit parameters BB, CC, and PP represent the $b\bar{b}$, $c\bar{c}$, and prompt dimuon contributions, respectively. The fit parameter BP (CP) estimates the number of events in which there is only one b (c) quark in the detector acceptance and the second lepton is produced by the decay or the misidentification of π or K mesons.

Component	No. of Events
BB	54583 ± 678
CC	24458 ± 1565
PP	41556 ± 651
BP	10598 ± 744
CP	10024 ± 1308
BC	2165 ± 693

previous inconsistencies between measurements and theoretical predictions of the correlated $b\bar{b}$ cross section.

However, a new problem arises that concerns the sample composition when the requirement that muons are accurately measured in SVXII detector is released. In order to have optimal impact parameter resolution, Ref. [6] uses very strict selection criteria, referred to as tight SVX selection in the following, by requiring muon tracks with hits in the first two layers of the SVXII detector, and at least in two of the remaining four outer layers. This requirement selects muon parent particles which decayed within a distance of $\simeq 1.5$ cm from the nominal beam line, or in other words inside the beam pipe. According to the simulation, approximately 96% of dimuons due to known SM processes, such as Drell-Yan, Υ, Z^0, and heavy flavor production, satisfy this latter condition. The efficiency of the SVX tight requirements for prompt dimuons is purely geometrical, and is measured to be 0.257 ± 0.004 by using $\Upsilon(1S)$ candidates [6]. For dimuons arising from heavy flavor production, the efficiency of the tight SVX selection is determined to be 0.237 ± 0.001 by using muons from J/ψ decays after reweighting their p_T distribution to be equal to that of muons from simulated decays of heavy flavors. The 7% decrease of the efficiency for heavy flavors is due to the fact that a small fraction of high-p_T b hadrons decay after the first SVXII layer. Figure 1 (a) shows the

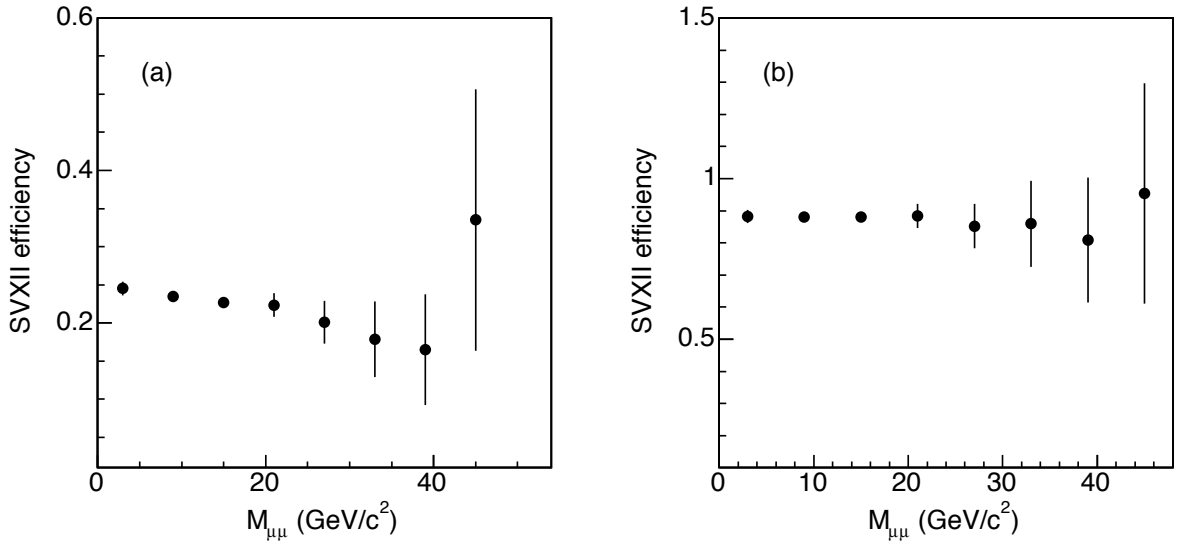

FIG. 1: Efficiency of SVX tight (a) and loose (b) selection in simulated dimuon events due to heavy flavor production (see text). The efficiency is shown as a function of the dimuon invariant mass.

efficiency of the tight SVX selection in simulated events due to heavy flavor production.

Analyses performed by the CDF collaboration customarily select tracks for secondary vertexing purposes with less draconian requirements such as tracks with hits in at least three out of the eight layers of the SVXII and ISL detectors (referred to as loose SVX selection in the following). The latter selection accepts muons from parent particles with a decay length as long as $\simeq 10.6$ cm. As shown by Fig. 1 (b), in this case the SVX selection efficiency is much higher and does not depend on the dimuon invariant mass. By using $\Upsilon(1S)$ and J/ψ candidates, we measure the efficiency of the loose SVX requirements to be 0.88 ± 0.01. The acceptance of the different SVX selections as a function of the decay length of the muon parent particle is verified by using cosmic muons that overlap in time with a $p\bar{p}$ collision (for this purpose we remove the request that the azimuthal angle between two initial muons be less than 3.135 radians). Cosmic muons, which are reconstructed as two back-to-back muons of opposite charge, cluster along the diagonal of the two-dimensional distribution of the muon impact parameters. As shown in Fig. 2, the loose SVX selection accepts larger decay lengths than the tight SVX selection. As shown by the scatter of the points along the $d_1 = d_2$ diagonal, both SVX selections yield rms impact parameter resolutions that are negligible on a scale of the order of centimeters.

If the dimuon sample before the tight SVX selection had the same composition of the

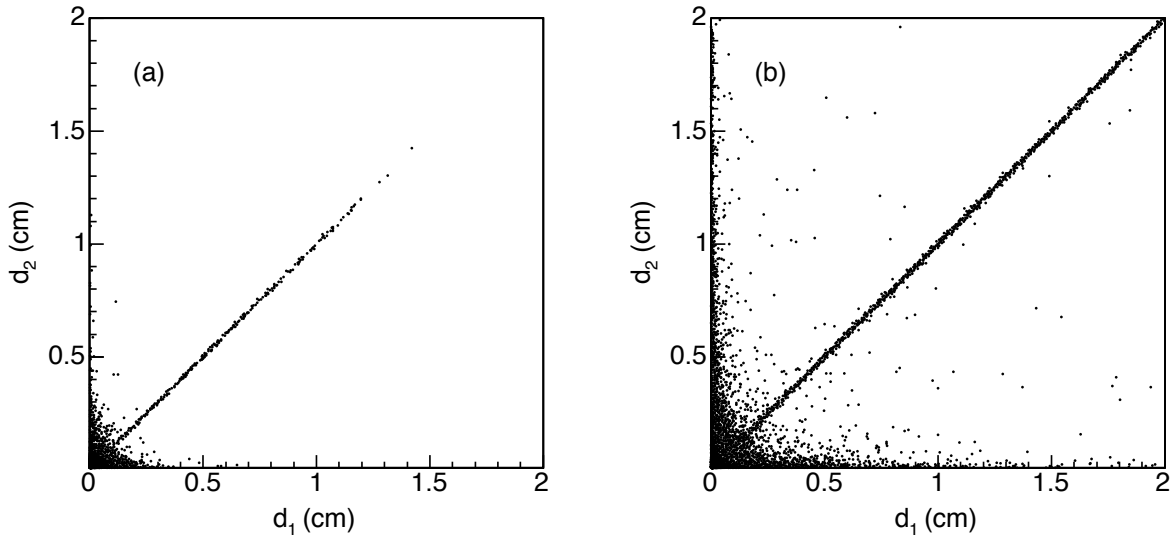

FIG. 2: Two-dimensional impact parameter distributions of muons that pass the (a) tight and (b) loose SVX requirements. Cosmic muons are reconstructed as two back-to-back muons of opposite charge and cluster along the $d_1 = d_2$ diagonal.

sample listed in Table I, the average efficiency of the tight SVX requirements in this data set would be 0.244 ± 0.002, whereas it is found to be 0.1930 ± 0.0004. This feature suggests the presence of an unexpected background, also referred to as the ghost contribution in the following, that is suppressed by the tight SVX selection because the data that pass this SVX selection are consistent with the NLO prediction. In the assumption that the contribution of the unexpected background to the dimuon sample selected with tight SVX requirements is negligible, its size is determined by the difference between the number of muon pairs in the data and the number of muons passing the tight SVX selection divided by the efficiency of the tight SVX requirements (see Table II). In Table II, the contribution of the unexpected background to dimuons that pass the loose SVX requirements is evaluated as the difference between the data and the number of events that pass the tight SVX requirements, divided by the efficiency of the tight SVX requirements and multiplied by that of the loose SVX requirements. The size of the unexpected background (153895 $\pm$ 4829 events) is is of a magnitude comparable to $b\bar{b}$ production (221564 $\pm$ 11615 events). When using the loose SVX requirements, the size of this unexpected background is reduced by a factor of two, whereas 88% of the dimuons due to known processes survive (the ghost size is 72553 $\pm$ 7264 events, whereas the $b\bar{b}$ contribution is 194976 $\pm$ 10221 events). In addition, dimuon

TABLE II: Number of events that pass different SVX requirements. QCD indicates the sum of the various components listed in Table I. Ghost indicates the additional background in the data. Dimuons are also split into pairs with opposite (OS) and same (SS) sign charge.

Type	No SVX	Tight SVX	Loose SVX
All	743006	143743	590970
All OS		98218	392020
All SS		45525	198950
QCD	589111 $\pm$ 4829	143743	518417 $\pm$ 7264
QCD OS		98218	354228 $\pm$ 4963
QCD SS		45525	164188 $\pm$ 2301
Ghost	153895 $\pm$ 4829	0	72553 $\pm$ 7264
Ghost OS		0	37792 $\pm$ 4963
Ghost SS		0	34762 $\pm$ 2301

pairs contributed by this background are equally split in opposite and same sign charge combinations.

The appearance of ghost events is not related to the instantaneous luminosity not to the presence of multiple interactions. We have investigated at length the possibility that ghost muons appear as originating outside the beam pipe because of pattern recognition problems in the SVX or COT detectors, and concluded that ghost events are real, not due to track reconstruction failures, and are different from QCD events. As an example, we compare yields of $D^0 \to K^-\pi^+$ (and charge-conjugate) decays in QCD and ghost events. We search for D^0 candidates by using tracks of opposite sign charge, with $p_T \geq 1.0$ GeV/c, $|\eta| \leq 1.1$, and contained in 60° cone around the direction of each initial dimuon. The two-track systems are constrained to arise from a common space point. Track combinations are discarded if the three-dimensional vertex fit returns a χ^2 per degree of freedom larger than 10 or if the vertex does not lay in the hemisphere containing the D^0 candidate. We attribute the kaon mass to the track with the same charge of the initial muon (RS combination, as expected for $B \to \mu^- D^0$ decays). We also study wrong sign combinations (WS) attributing the kaon mass to the track with opposite charge as the muon. A D^0 signal found in the

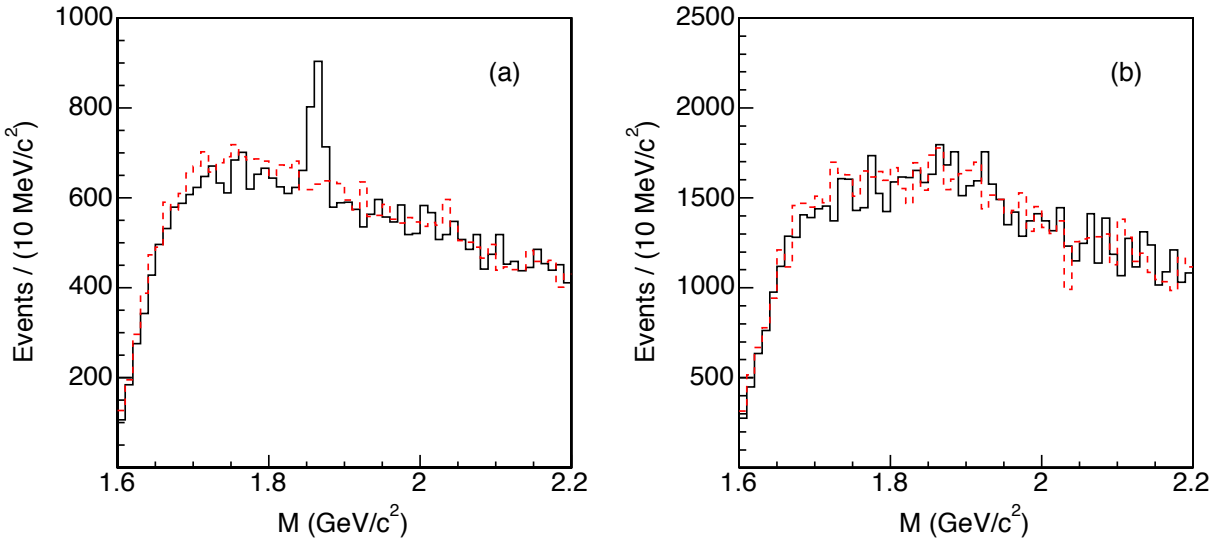

FIG. 3: Invariant mass, M, distributions of RS (histogram) and WS (dashed histogram) D^0 candidates in (a) QCD and (b) ghost events.

WS combinations is a measure of the fraction of fake muons in QCD events due to b- and c-quark production, whereas a D^0 signal in RS combinations found in ghost events would indicate a heavy flavor contribution. The invariant mass distribution in Fig. 3 confirms that ghost events do not contain an appreciable amount of heavy flavors.

The unnoticed presence of a ghost contribution of this size, that is incrementally reduced by stricter SVX requirements, can help explain all the inconsistencies mentioned in the introduction. The general observation is that the measured $\sigma_{b\to\mu,\bar{b}\to\mu}$ increases as the SVX requirements are made looser and is almost a factor of two larger than that measured in [6] when no SVX requirements are made [8]. As mentioned above, the magnitude of the ghost contribution is comparable to the $b\bar{b}$ contribution when no SVX selection is made and in combination would account for the measurement reported in [8]. Similarly, for the loose SVX criteria, the magnitude of the ghost contribution, when added to the expected $b\bar{b}$ contribution of 194976 ± 10221 events, coincides with the cross section measurement reported in [7] and the $\bar{\chi}$ value reported in [4] since these measurements use similar sets of silicon criteria.

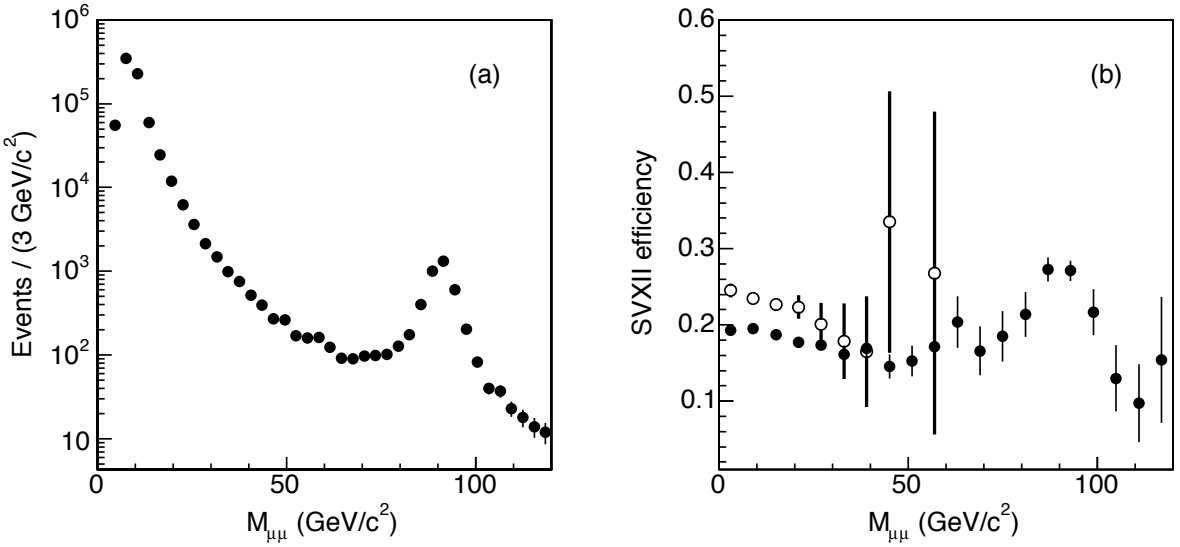

FIG. 4: Invariant mass distribution (a) of the dimuon pairs used in the study. The efficiency (b) of the tight SVX requirements as a function of the dimuon invariant mass in the data (•) is compared to that in the heavy flavor simulation (◦).

A. SM sources of ghost events

In the following, we investigate several possible sources of the unexpected background that might have been not properly accounted for by previous experiments. Possible sources are: (a) heavy flavored hadrons with an unexpectedly large Lorentz boost; (b) decays of particles with a lifetime longer than that of heavy flavors, such as K, π, and K^0_S mesons, and hyperons; (c) or secondary interactions that occur in the detector volume. Figure 4 plots the invariant mass of dimuon pairs before the tight SVX selection, and the efficiency of this selection as a function of the dimuon invariant mass. The efficiency of tight SVX requirements in the data is below that in the heavy flavor simulation only for dimuon invariant masses smaller than 40 GeV/c^2, and then rises to the expected value of 0.257 where events are mostly contributed by prompt Z^0 decays. This feature does not favor the first hypothesis (a).

A long-lived particle contribution is suggested by the comparison of the impact parameter distribution of dimuons that pass the loose and tight SVX requirements. The request that muons pass loose SVX requirements is momentarily used to reduce the possible contribution of muons arising from interactions that occur beyond the SVXII detector. We note that loose SVX requirements sculpt the impact parameter distribution of muons arising from

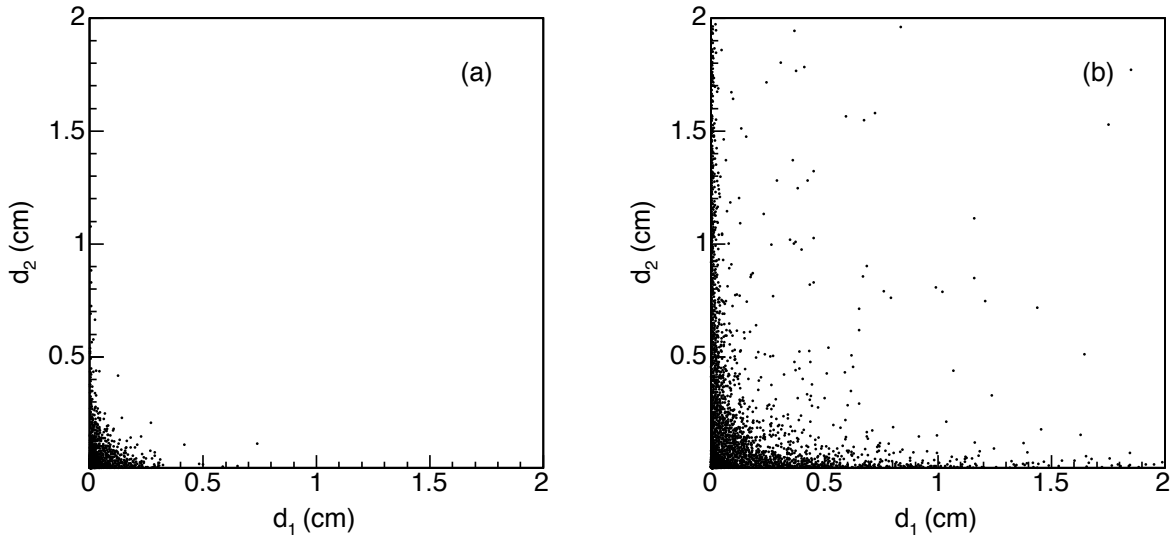

FIG. 5: Two-dimensional impact parameter distribution of dimuons that pass the (a) tight and (b) loose SVX requirements.

the decay of objects with a lifetime much longer than that of B hadrons, such as π, K, or K^0_S mesons. Two-dimensional impact parameter distributions are shown in Fig. 5. One-dimensional distributions are shown in Fig. 6. The impact parameter distribution of muons in ghost events is completely different to that of the QCD contribution. According to the heavy flavor simulation [6], dimuons with impact parameter larger than 0.12 cm only arise from $b\bar{b}$ production. We fit the impact parameter distribution in Fig. 7 with the function $A\exp(-d/(c\tau))$ in the range $0.12 - 0.4$ cm. The best fit returns $c\tau = 469.7 \pm 1.3$ μm in agreement with the value 470.1 ± 2.7 μm expected for the b-hadron mixture at the Tevatron [5]. We conclude that the data sample selected with the tight SVX selection is not appreciably contaminated by the unexpected background. This supports our procedure for estimating the ghost size by assuming that the ghost contribution to events selected with tight SVX requirements is negligible. It also follows that the $b\bar{b}$ contribution to dimuons with impact parameter larger than 0.5 cm is negligible.

In ghost events, the presence of a large tail extending to high impact parameters suggests the contribution of particles with a lifetime much longer than that of b quarks, such as K^0_S, K and π mesons, and hyperons. We first investigate muons produced by pion and kaon in-flight-decays. As reported in Ref. [6], after having selected muon pairs with the tight SVX requirements, approximately 30% of the QCD contribution contains muon signals

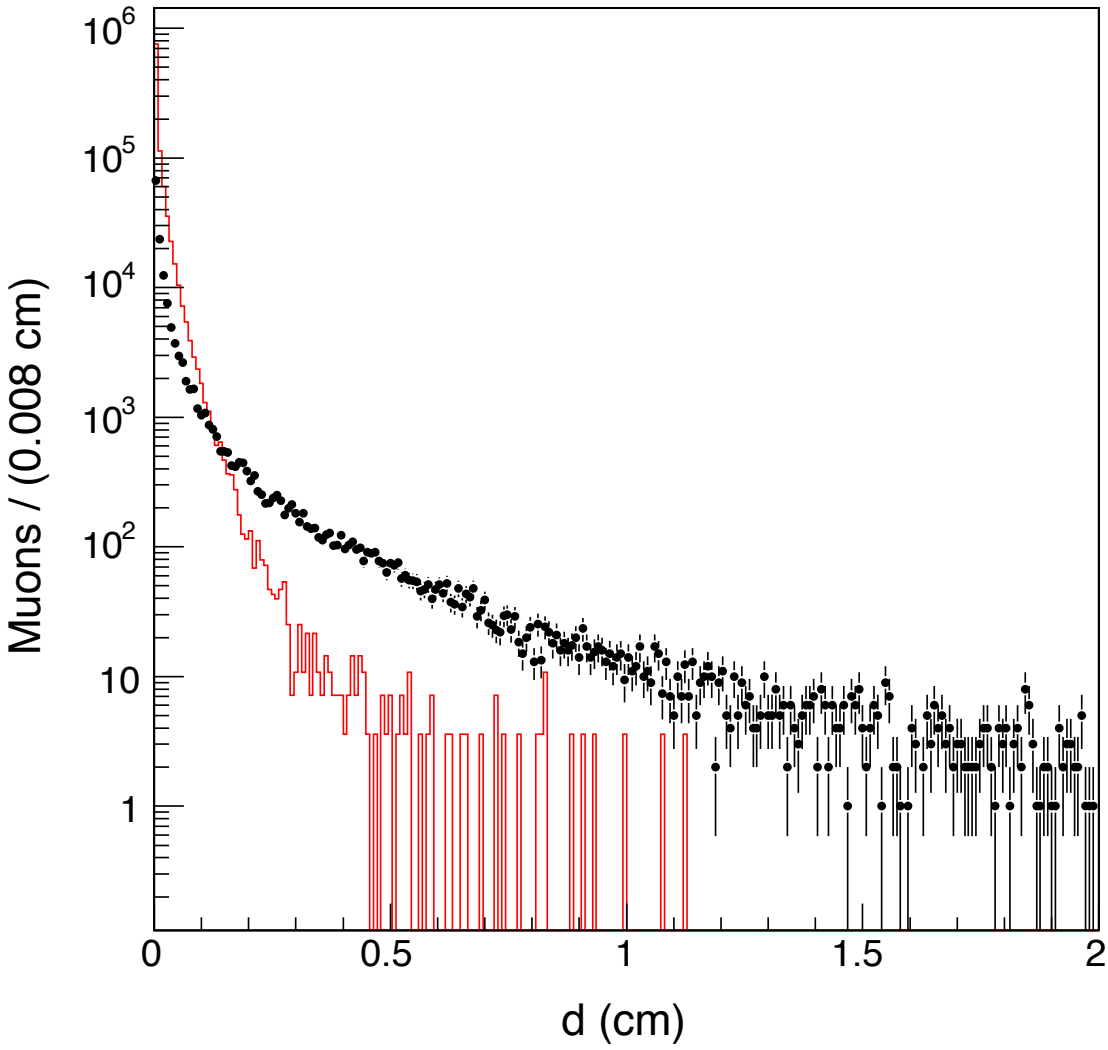

FIG. 6: Impact parameter distribution of muons contributed by ghost (•) and QCD (histogram) events. Muon tracks are selected with loose SVX requirements. The detector resolution is $\simeq 30$ μm, whereas bins are 80 μm wide.

mimicked by prompt hadronic tracks. The size of the unexpected background has been estimated assuming that the efficiency of the tight SVX requirements for these tracks is the same as that for real muons. This is certainly true when fake muons are generated by hadronic punchthroughs. However, muons arising from π or K decays that happen inside the tracking volume may yield misreconstructed tracks that are linked to hits in the SVXII detector less efficiently than real muons. We estimate the size of this contribution

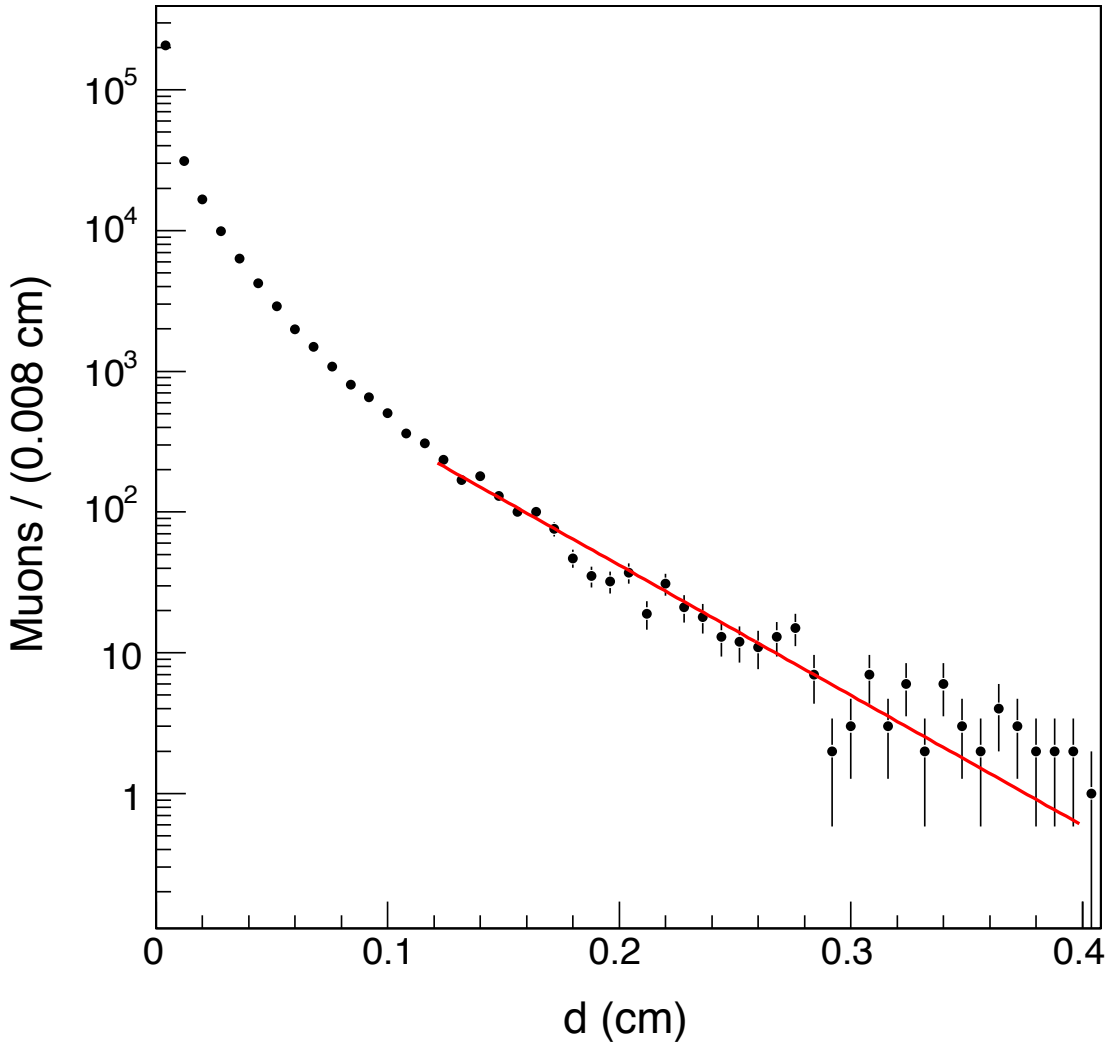

FIG. 7: Impact parameter distribution of muons that pass the tight SVX requirements. The line represents the fit described in the text.

by using pions and kaons produced in the large statistics heavy flavor simulation used to derive the dimuon acceptance for the $\sigma_{b\to\mu,\bar{b}\to\mu}$ measurement [6]. We use the quantity $\Delta^2 = 1/3\cdot[(\eta^h-\eta^{\rm track})^2/\sigma_\eta^2+(\phi^h-\phi^{\rm track})^2/\sigma_\phi^2+(1/p_T^h-1/p_T^{\rm track})^2/\sigma_{1/p_T}^2]$ to measure the difference between the momentum vectors of the undecayed pions or kaons (h) and that of the closest reconstructed tracks [3]. Figure 8 shows the Δ distribution as a function of R, the decay

[3] The experimental resolutions are $\sigma_\phi = \sigma_\eta = 10^{-3}$ rad and $\sigma_{1/p_T} = 2\cdot 10^{-3}$ (GeV/c)$^{-1}$.

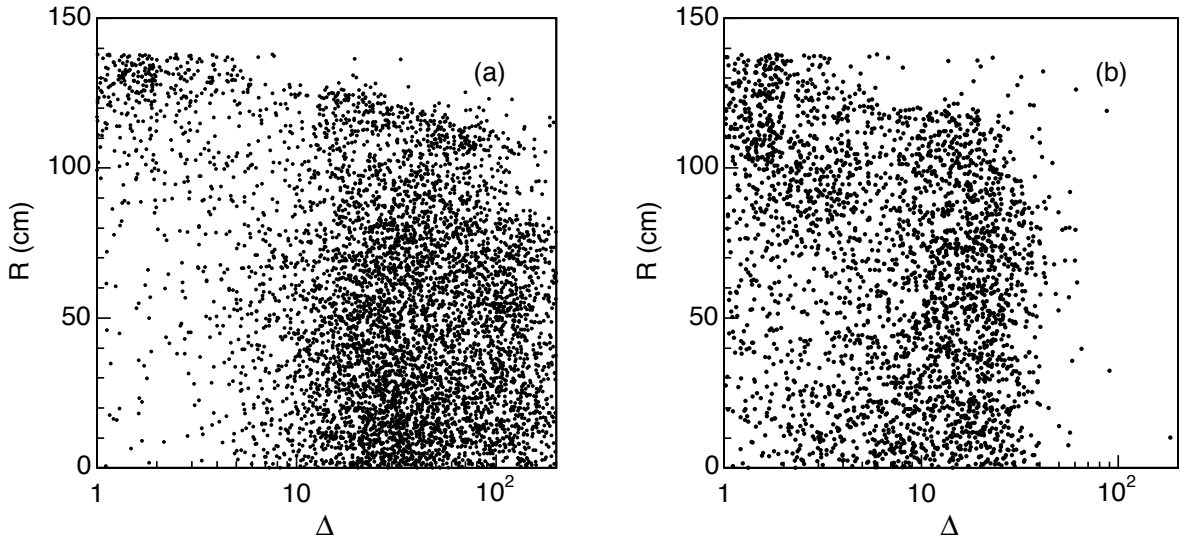

FIG. 8: Distribution of Δ (see text) as a function of the distance R of the (a) K and (b) π decay vertices from the beamline. For comparison, the analogous distribution for real muons from heavy flavor decays does not extend beyond $\Delta = 9$.

TABLE III: Number of pions and kaons corresponding to a reconstructed track with $p_T \geq 3$ GeV/c and $|\eta| \leq 0.7$, that decay inside the tracking volume, produce CMUP muons with a L1 primitive, and pass different SVX selections.

Selection	π	K
Tracks	2667199	1574610
In-flight-decays	14677	40561
CMUP+L1	1940	5430
Loose SVX	897	3032
Tight SVX	319	1135

distance from the beamline. One notes that most of the decays that happen at radial distances $R \leq 120$ cm yield misreconstructed tracks. The fractions of in-flight-decays that produce CMUP muons with $p_T \geq 3$ GeV/c, a L1 primitive, and pass different SVX selections are listed in Table III. The contributions of muons due to in-flight-decays is evaluated

using simulated events produced by generic parton hard scattering [4]. In the simulation, there are 44000 track pairs per CMUP pair due to $b\bar{b}$ production with the same kinematic acceptance ($p_T \geq 3$ GeV/c and $|\eta| \leq 0.7$). The ratio of the number of pions to that of kaons is approximately 5/1. Each simulated track in the kinematic acceptance is weighted with the corresponding in-flight-decay probabilities of producing CMUP muons listed in Table III. Tracks are also weighted with the probabilities, measured in Ref. [6], that π or K punchthrough mimics a CMUP signal. In the latter case, the efficiency of the SVX requirement is the same as for real muons, and we disregard the cases in which both muons arise from hadronic punchthrough. Having normalized this simulation to the number of observed initial muons arising from $b\bar{b}$ production, we predict a contribution to ghost events due to in-flight-decays of pions and kaons that is 57000 events, 44% and 8% of which pass the loose and tight SVX selection, respectively. In the 25000 fake dimuon events that pass the loose SVX selection, approximately 15000 muons arise from kaon in-flight-decays. This prediction depends on how well the HERWIG generator models generic parton hard scattering and its uncertainty is difficult to estimate. Figure 9 shows the impact parameter distribution of muons arising from in-flight-decays of pions and kaons produced in simulated $b\bar{b}$ and $c\bar{c}$ events. The number of events in Fig. 9 has to be multiplied by a factor of five in order to be compared with the data in Fig. 6. Our estimate of the number of muons arising from in-flight-decays accounts for 35% of the ghost muons, but for less than 10% of those with $d \geq 0.5$ cm.

In addition, muons in ghost events can be mimicked by the punchthrough of hadrons arising from the decay of K^0_S mesons or hyperons. We have searched the dimuon data set for $K^0_S \to \pi^+\pi^-$ decays in which a pion punchthrough mimics the muon signal. We combine all initial muons with all opposite sign tracks with $p_T \geq 0.5$ GeV/c contained in a 40° cone around the direction of the initial muons. Muon-track combinations are constrained to arise from a common space point. They are discarded if the three-dimensional vertex fit returns a χ^2 per degree of freedom larger than 10. Figure 10 (a) shows the invariant mass distribution of the K^0_S candidates. A fit of the data with a Gaussian function to model the signal plus a second order polynomial to model the background yields a signal of 5348 ± 225 K^0_S mesons.

[4] We use option 1500 of the HERWIG program to generate final-state partons with transverse momentum larger than 3 GeV/c [6].

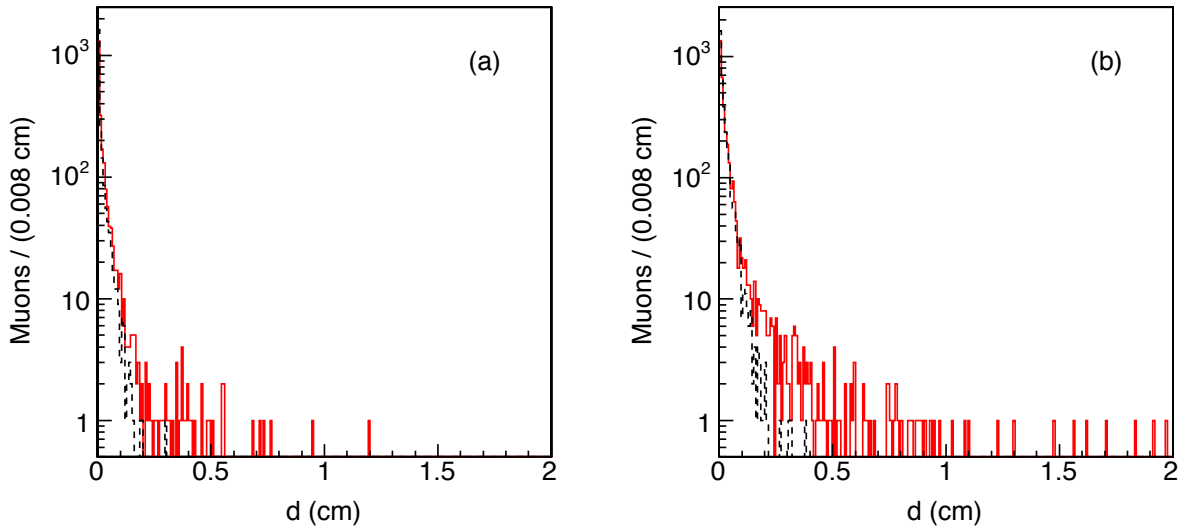

FIG. 9: Impact parameter distributions of simulated CMUP muons (histogram) that pass all analysis requirements, including the loose SVX selection, and arise from (a) pions and (b) kaon in-flight decays. The dashed histograms show the impact parameter of the parent pions and kaons.

The impact parameter distribution of initial muons produced by K^0_S decays is shown in Fig. 10 (b). The data also contain a smaller number of cases in which the initial muon is mimicked by the products of hyperon decays. Using a similar technique, we have searched the data for $\Lambda \to p\pi^-$ decays and we find a signal of 678 ± 60 Λ baryons.

The contribution of muons produced in secondary interactions in the detector volume has been investigated using the data. We search for secondary interactions by combining initial muons with all tracks with $p_T \geq 1$ GeV/c contained in a 40° cone around the muon direction. Muon-track combinations are constrained to arise from a common space point. They are discarded if the three-dimensional vertex fit returns a χ^2 per degree of freedom larger than 10. The distribution of R, the distance of a reconstructed secondary vertex from the detector origin in the plane transverse to the beam line, is shown in Fig. 11. The distance R is negative when the secondary vertex is in the hemisphere opposite to that containing the momentum of the muon-track system. Secondary interactions are characterized by spikes at R values where the detector material is concentrated, such as SVX supports or the COT can. From the absence of spikes we conclude that the contribution of secondary interactions to initial muons in ghost events is negligible.

Our estimate of the size of possible sources of unexpected events underpredicts the amount

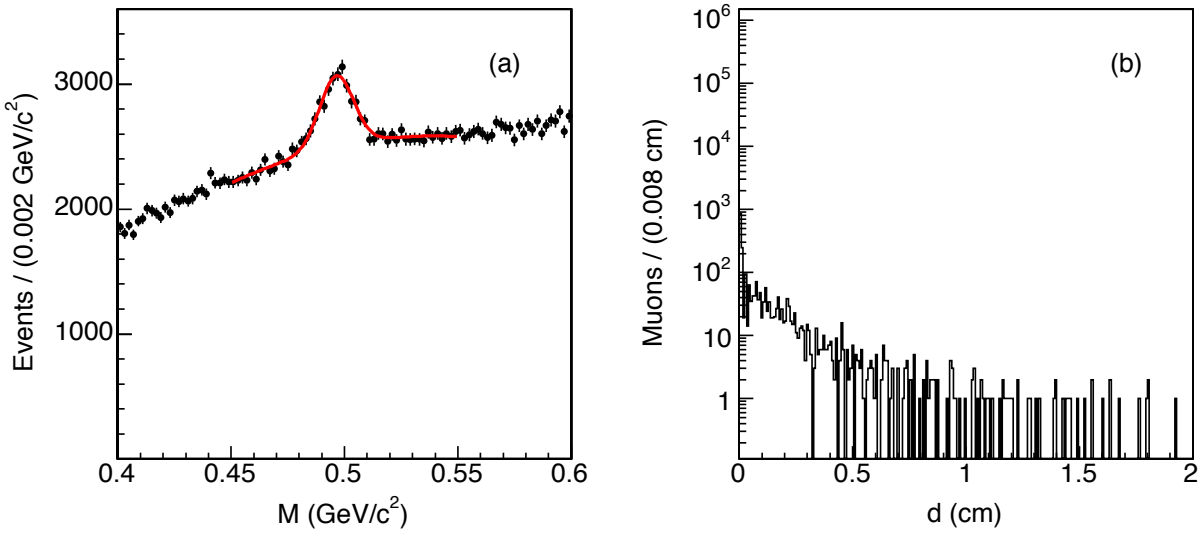

FIG. 10: Distributions of (a) the invariant mass of pairs of initial muons and opposite sign tracks and of (b) the impact parameter of initial muons, produced by K^0_S decays, that pass the loose SVX selection. The solid line represents a fit described in the text. In the impact parameter distribution, the combinatorial background is removed with a sideband subtraction method. For comparison, the vertical scale in (b) is kept the same as in Fig. 6.

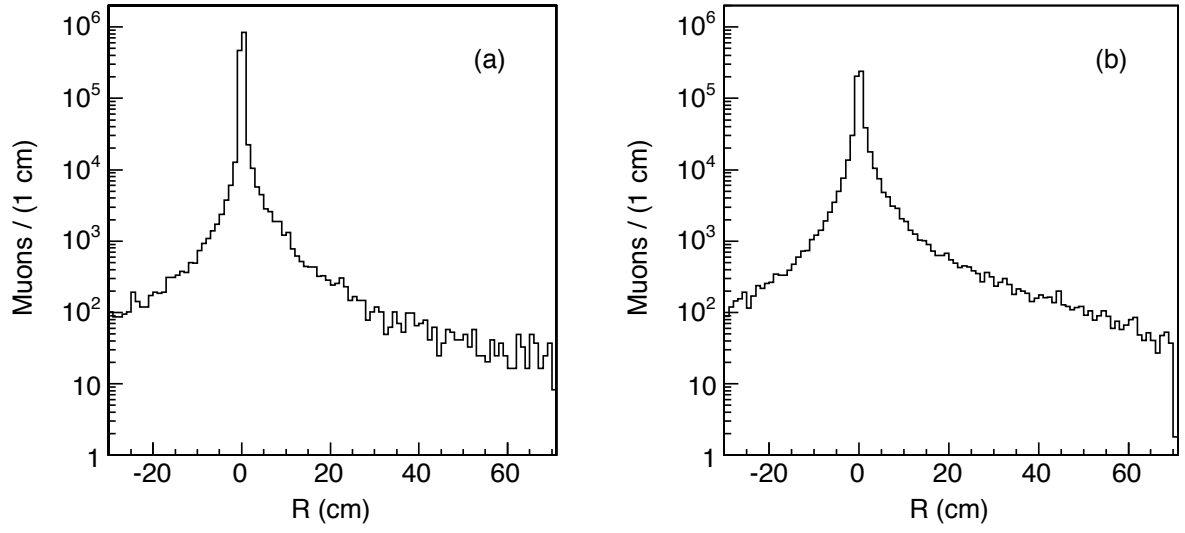

FIG. 11: Distributions of R, the signed distance of muon-track vertices from the nominal beam line for (a) QCD and (b) ghost events (see text).

of ghost events. Given the possible large uncertainty of the in-flight-decay prediction, we also cannot rule out that the unexpected background can be completely accounted by a combination of all effects mentioned above. However, were the unexpected background all due to these sources, it is not expected to contain a significant number of additional real muons. Therefore, it cannot be the origin of the excess of low-mass dileptons reported in Ref. [3]. That study is repeated in the next section.

V. STUDY OF EVENTS THAT CONTAIN AN ADDITIONAL MUON

We search events that contain a pair of initial muons, which pass our analysis selection without any SVX requirement, for additional tracks with $p_T \geq 2$ GeV/c and a matching stub in the CMU, CMX, or CMP muon detectors (the three detectors cover the pseudorapidity region $|\eta| \leq 1.1$). For muons with $p_T \geq 2$ GeV/c and $|\eta| \leq 1.1$, the muon detector efficiency in the heavy flavor simulation is 0.805 ± 0.008. We measure the muon detector efficiency in the data by using J/ψ candidates acquired with the μ-SVT trigger (see Ref. [6] for more details). After reweighting the kinematic of the muons from J/ψ decays to model that of simulated muons from heavy flavor decays we measure the efficiency of the muon detector in the data to be 0.838 ± 0.004.

According to the heavy flavor simulation, additional real muons can only arise from sequential decays of single b hadrons (the $g \to b\bar{b}$ and $g \to c\bar{c}$ contributions are suppressed by the request of two initial muons with $p_T \geq 3$ GeV/c, $|\eta| \leq 0.7$, and invariant mass larger than 5 GeV/c^2). In addition, one expects a contribution of additional muons due to hadrons mimicking the muon signal. In the data, 9.7% of the dimuon events contain an additional muon (71835 out of 743006 events). In events containing an $\Upsilon(1S)$ candidate, that are included in the dimuon sample, the probability of finding an additional muon is $(0.90 \pm 0.01)\%$. As shown in Fig. 12, only 94 ± 41 events with an identified K^0_S meson, $(1.7 \pm 0.8)\%$ of the total, contain an additional lepton.

Our investigation starts by simply measuring the efficiency of the tight SVX requirements for initial muon pairs in events that contain additional muons. The efficiency drops from 0.193 to 0.166 (see Fig. 13). This is the opposite of what one would expect if all the unexpected background were due to dimuons arising from π or K decays, or secondary interactions in the detector volume, because these processes are not expected to produce

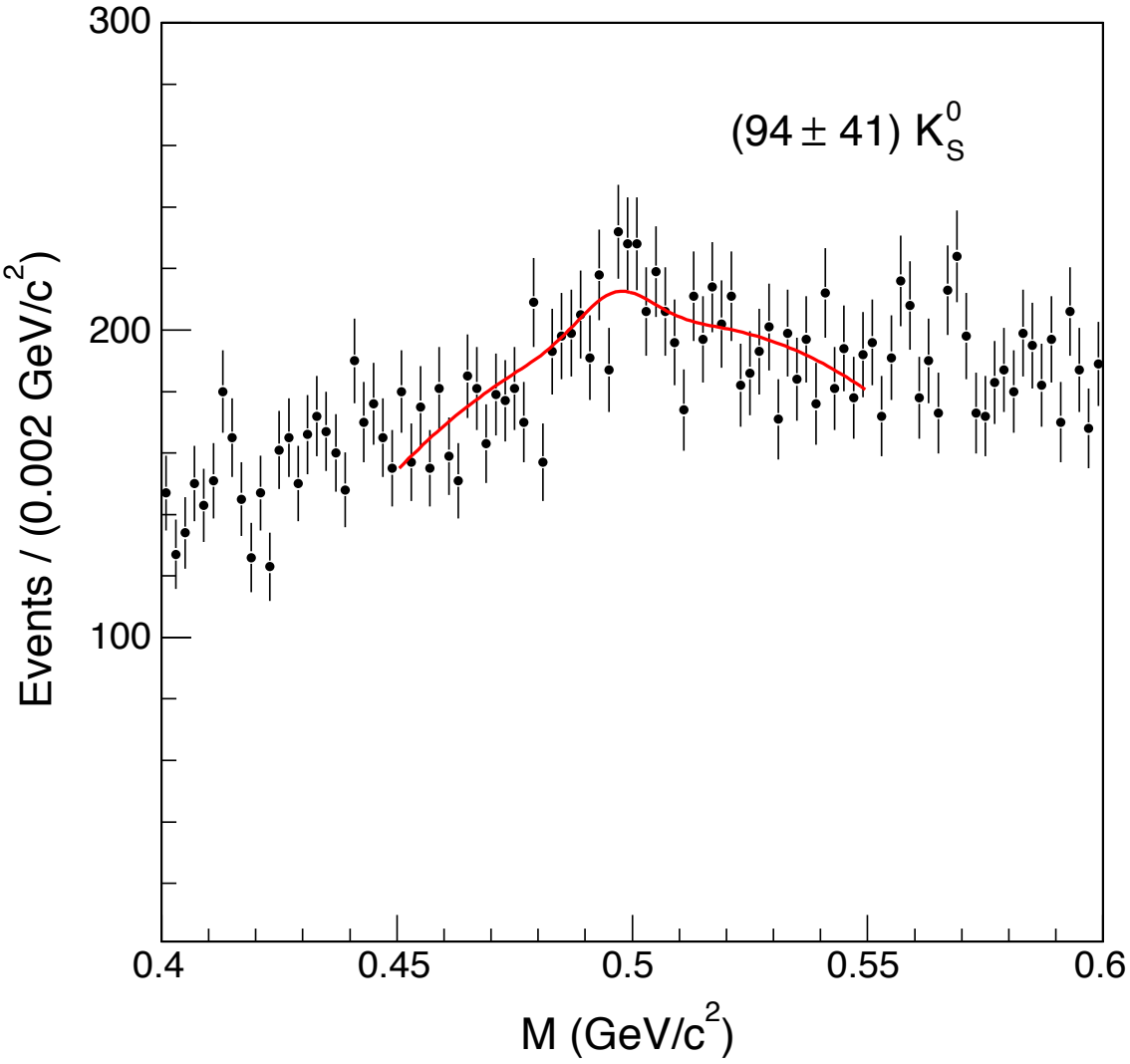

FIG. 12: Distribution of the invariant mass of pairs of initial muons and opposite sign tracks in events that contain an additional muon.

more additional muons than $\Upsilon(1S)$ or K^0_S production. This simple observation anticipates that a fraction of the ghost events is quite special because it also contains more additional muons than QCD events.

Following the study in Ref. [3], additional muons are paired with one of the initial muons if their invariant mass is smaller than 5 GeV/c^2. For this study, we use a larger statistics data sample [5]. Following the analysis procedure of Ref. [3], we retain muon combinations with

[5] The correlated $b\bar{b}$ cross section measurement uses 742 pb^{-1} of data in which the dimuon trigger is not

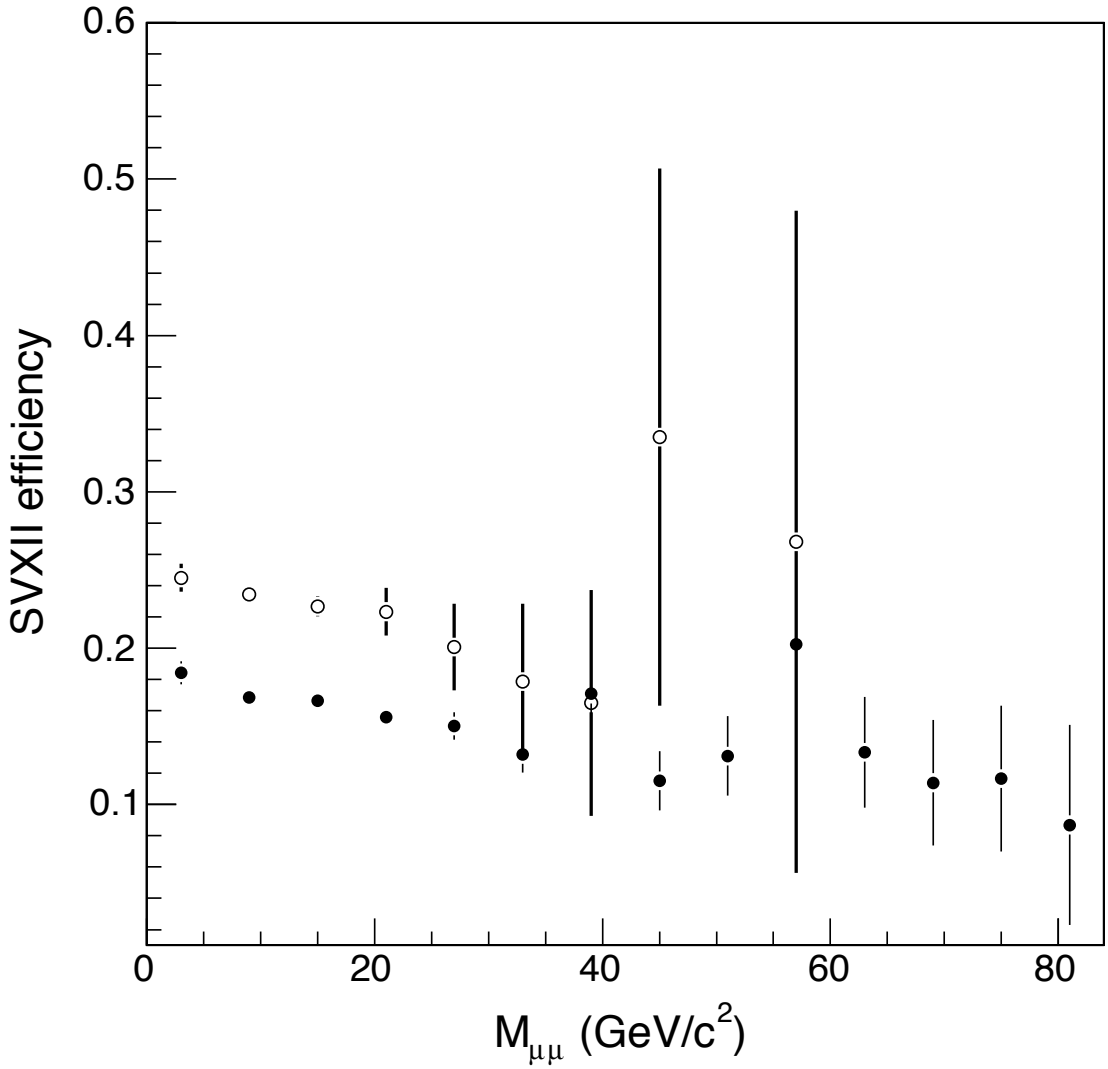

FIG. 13: The efficiency of the tight SVX requirements as a function of the initial-dimuon invariant mass in the data (•) is compared to that in the heavy flavor simulation (◦). The events contain one or more additional muon without any SVX requirement.

charges of opposite sign (OS). As in Ref. [3], we estimate the contribution of fake muons from the number of observed same sign (SS) muon pairs. We use this procedure since initial prompt dimuons are not simulated. In the case of Drell-Yan or quarkonia production, fake additional muons arise from the underlying event and one expects no charge correlation

prescaled as a function of the instantaneous luminosity. From the rate of dimuon events that pass the analysis selection, the luminosity of the larger data sample is estimated to correspond to 1426 pb^{-1}.

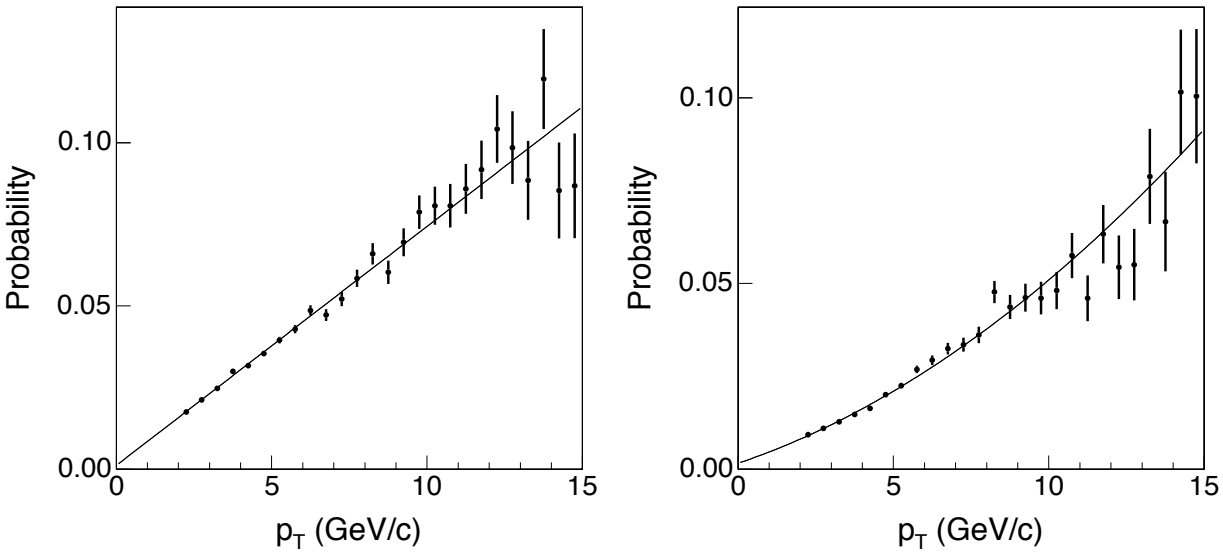

FIG. 14: Probability that a track with $|\eta| \leq 1.1$ mimics a muon signal in the CMU, CMX, or CMP detectors as a function of the kaon (left) or pion (right) transverse momentum. We have verified that these fake probabilities do not depend on the SVX requirements applied to the tracks.

between initial and additional fake muons. However, in the simulation of heavy flavor decays, one finds more OS than SS tracks surrounding an initial muon. These tracks come from the b- and c-quark fragmentation and decay. In the simulation, the ratio of OS to SS combinations as well as the ratio of the numbers of pion to kaon tracks is a function of the invariant mass of the muon-track pair. We evaluate the fake muon contribution by weighting pion and kaon tracks in the heavy flavor simulation with the probability that hadronic punchthrough mimics a muon signal. These fake probabilities as a function of the track p_T are shown in Fig. 14. These probabilities have been measured in the data using a sample of $D^0 \to K^-\pi^+$ decays acquired with the CHARM and μ-SVT triggers. The procedure for determining these probabilities is described in detail in Appendix B of Ref. [6].

The rate of real plus fake muon pairs with small invariant mass is evaluated after rescaling the parton level cross section predicted by the HERWIG generator to match the measurements $\sigma_{b\to\mu,\bar{b}\to\mu} = 1549 \pm 133$ pb and $\sigma_{c\to\mu,\bar{c}\to\mu} = 624 \pm 104$ pb [6]. The simulation prediction is also evaluated subtracting SS from OS combinations due to either real or fake muon pairs. In the simulation, the initial pair of muons is always arising from b-quark semileptonic decays. However, in the data, only 91% of the initial muons recoiling against a small mass dimuon pair is due to real heavy flavor (relative size of the BB and BP components in Table I). In

addition, 2% of these recoiling muons are mimicked by hadrons from heavy flavor decays [6]. We account for this by increasing the rates predicted by the simulation by a factor of 1.12.

Figure 15 shows the ratio of the total number of $OS - SS$ muon pairs predicted by the above calculation to that of real $OS - SS$ dimuons from heavy flavor decays. The fake contribution is approximately 33% of that of real muons from sequential decays of single b quarks. Figure 16 compares the invariant mass spectrum of $OS - SS$ muon pairs in the data and the heavy flavor simulation. Since the simulation is effectively normalized to the observed number of initial muon pairs, the prediction has a 3% systematic error due to the branching ratio $b \to c \to \mu$ plus a 3% uncertainty due to the absolute pion and kaon rates predicted by the simulation [6] (the systematic uncertainty of the muon detector efficiency is negligible). This systematic uncertainty is not shown in Fig. 16. This figure shows that the number of J/ψ mesons in the data is correctly modeled by the simulation in which J/ψ mesons only arise from $b\bar{b}$ production. The agreement between the number of observed and predicted J/ψ mesons selected without any SVX requirement supports the estimate of the efficiency of the tight SVX requirement and the resulting value of the correlated $b\bar{b}$ cross section reported in Ref. [6]. However, as already noticed in Ref. [3], the data are underestimated by the simulation for invariant masses smaller than 2 GeV/c^2. The excess of 8451 ± 1274 events results from an observation of 37042 ± 389 and a prediction of 28589 ± 1213 events. The size and shape of the excess is consistent with what was first reported in Ref. [3], in which the excess was mostly observed in a high statistics $e\mu$ sample. We have an advantage with respect to the previous observation. The robustness of the prediction can be verified by comparing the observed and predicted invariant mass spectrum of dimuon pairs when the initial muons are selected with the tight SVX requirements. In this case we observe 6935 ± 154 events, whereas 6918 ± 293 are predicted. The corresponding invariant mass distribution is shown in Fig. 17.

A. Kinematics of additional muons in ghost events

The excess of 8451 ± 1274 $OS - SS$ pairs with invariant mass smaller than 5 GeV/c^2 does not represent the number of additional muons contained in the unexpected background. It is a measure of the charge asymmetry of additional muons as they get closer to the initial muon with which they are combined. For 1,426,571 initial dimuons, we find 94148 OS and

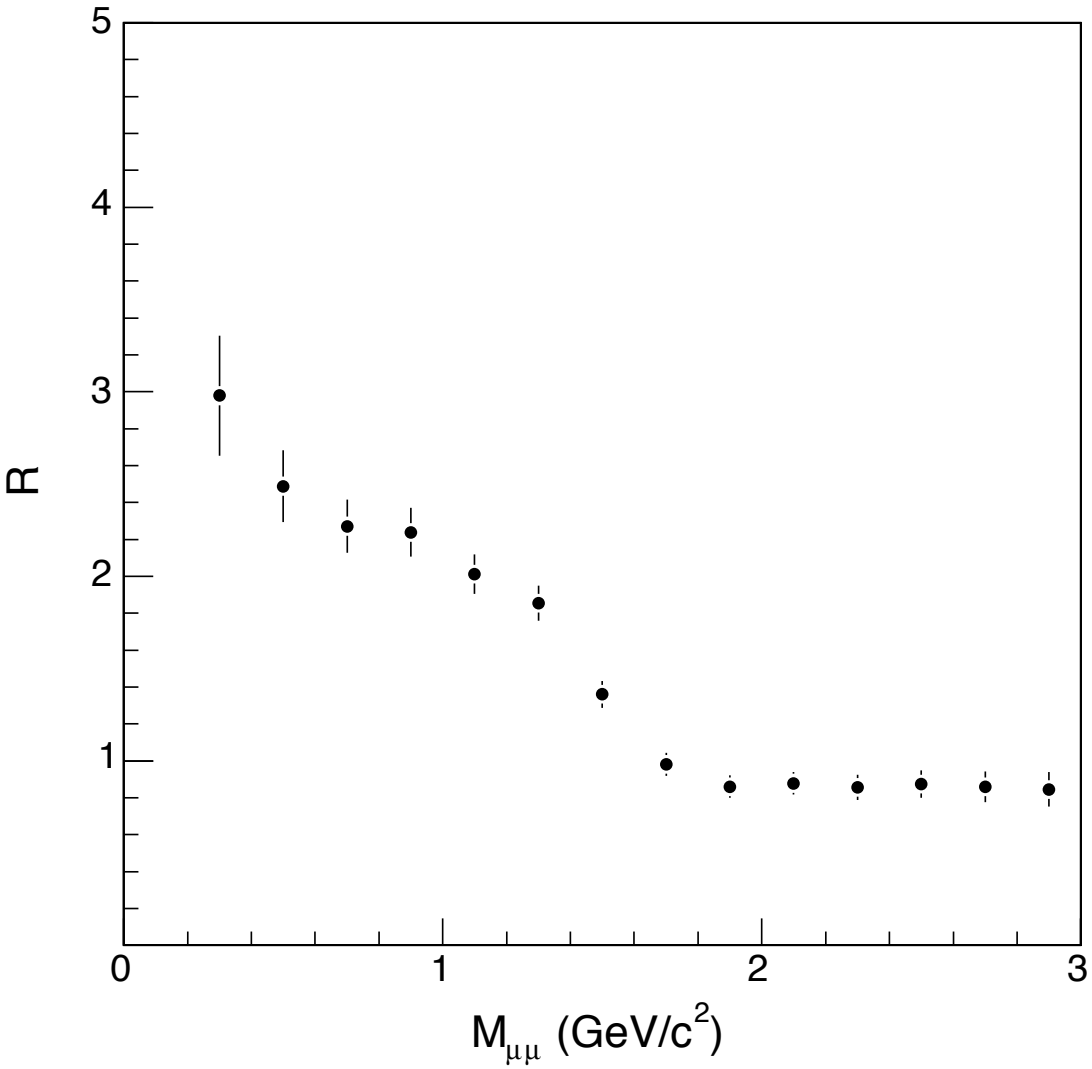

FIG. 15: Ratio R of total number of $OS - SS$ muon pairs to that of real $OS - SS$ pairs arising from heavy flavor decays as a function of the dimuon invariant mass. We use simulated events generated with the HERWIG Monte Carlo program. The generator parton-level cross sections have been scaled to match the data [6]. The number of fake muon pairs has been evaluated by weighting simulated hadronic tracks with the probability of mimicking a muon signal as measured with data. Errors are statistical only.

57106 SS combinations with an additional muon with $m_{\mu\mu} \leq 5$ GeV/c^2. A rough calculation predicts that 14200 SS and OS fake muon combinations are produced by the underlying

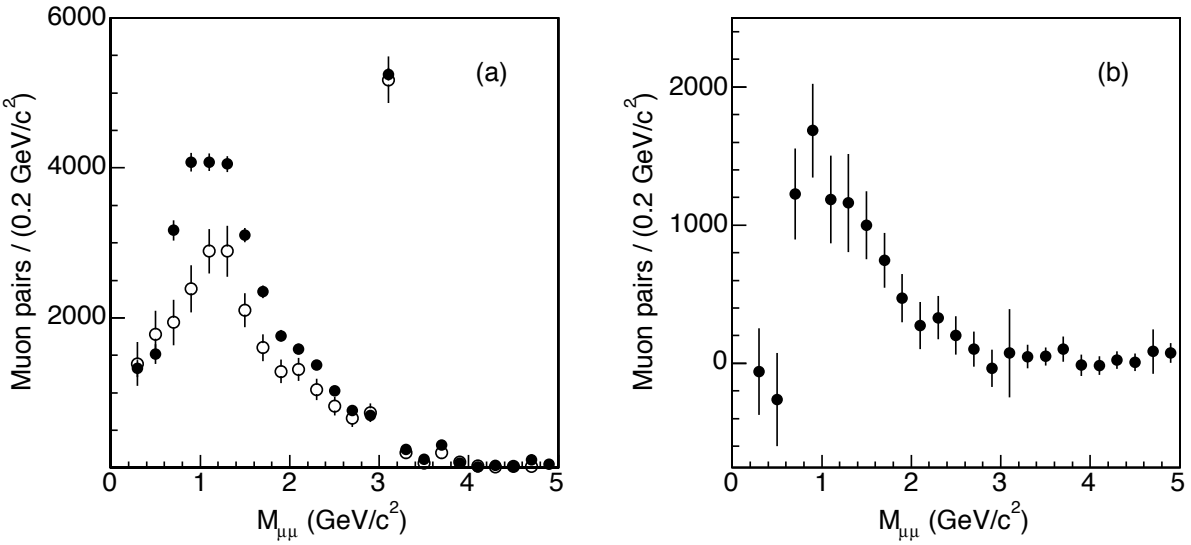

FIG. 16: The invariant mass distribution of (a) $OS - SS$ muon pairs in the data (•) is compared to the simulation prediction (○). One of the two initial muons in the event is combined with an additional muon if their invariant mass is smaller than 5 GeV/c^2. The difference (b) between data and prediction is also shown.

event [6]. The heavy flavor simulation, that also accounts for fake muons, predicts 40899 OS and 12309 SS real plus fake combinations for a grand total of 55100 OS and 26500 SS pairs. This simple prediction underestimates the data by 39000 OS and 30500 SS pairs. The contribution of the unexpected background to OS and SS pairs can be better determined from the difference between the data and the QCD expectation. The QCD expectation is the number of muon combinations found in events in which the initial dimuons pass the tight SVX requirements divided by the SVX requirement efficiency. This study is summarized in Table IV. For the unexpected background, the fraction of events that carries an additional real or fake muon with any charge is $(15.8 \pm 0.3)\%$, which is approximately a factor of two higher than in QCD events. The fraction of additional muons due to tracks mimicking a muon signal is estimated in the next section.

In order to compare with the previous measurement [3], we have analyzed dimuon pairs with $m_{\mu^+\mu^-} \leq 5$ GeV/c^2. This requirement is appropriate for selecting dimuons produced by sequential semileptonic decays of single b-quarks, but could bias the investigation of the

[6] These numbers are derived from the 1% probability of finding an additional muons in events with $\Upsilon(1S)$ candidates and assuming that the underlying event is the same for all processes.

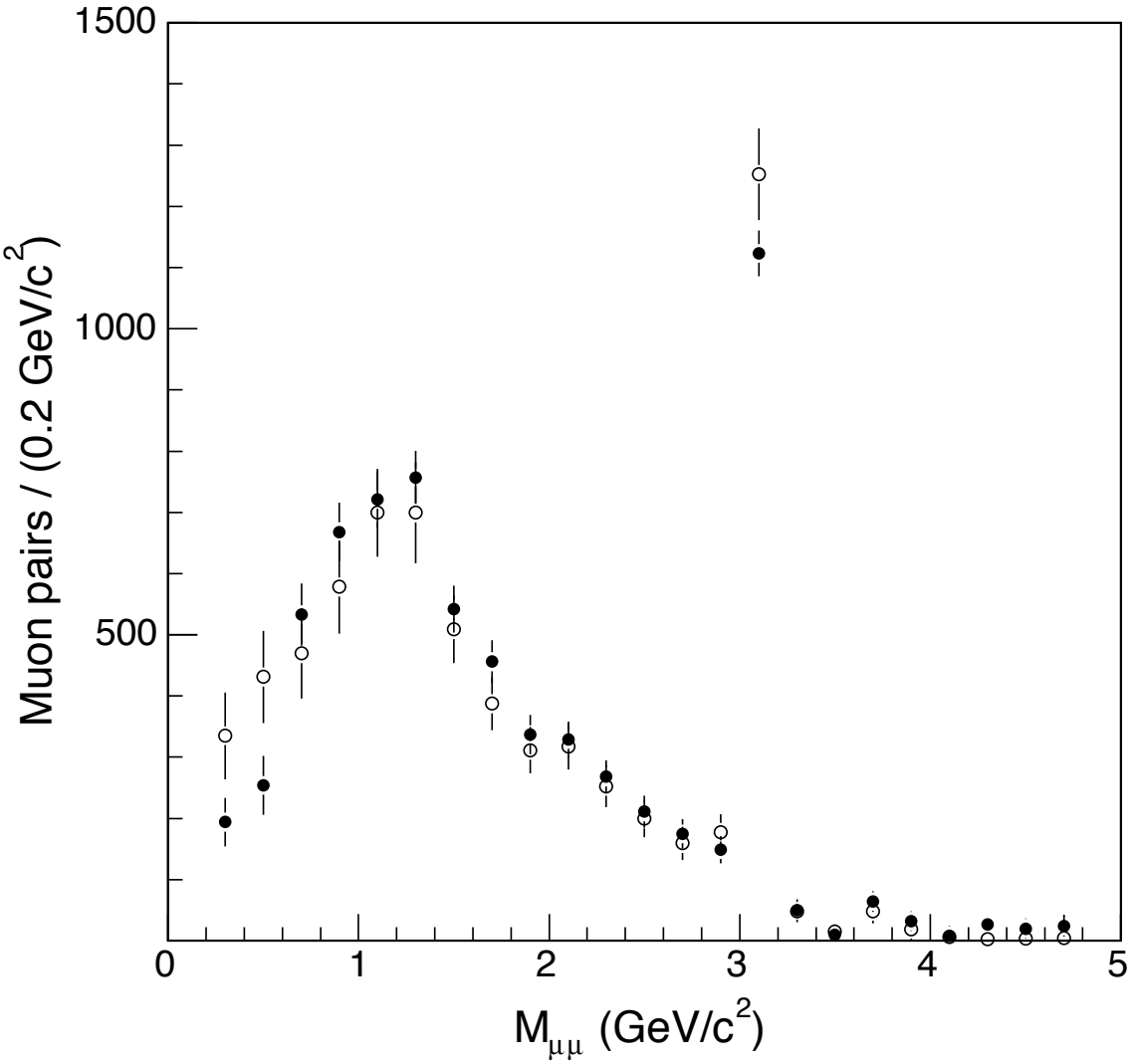

FIG. 17: The invariant mass distribution of $OS - SS$ muon pairs in the data (•) is compared to the simulation prediction (○). Initial muons are selected using the tight SVX requirements.

unexpected background. Therefore, we search dimuon events for additional muons without any invariant mass cut. If the initial dimuon pair has opposite charge, we combine the additional muon with the initial muon of opposite charge (OSO combinations). If the initial muons have same sign charge, we randomly combine the additional muon with one of the initial muons (SSO and SSS combinations). The QCD contribution is estimated as the number of combinations in events in which initial dimuons pass the tight SVX requirements (SVX contribution) divided by the efficiency of the tight SVX requirements. As usual,

TABLE IV: Number of events as a function of N_c, the number of combinations of initial and additional muons. Additional muons are combined with initial muons if the invariant mass is smaller than 5 GeV/c^2. The numbers of events with at least one combination are split according to opposite (OS) or same (SS) charge sign. "SVX" are numbers of events that pass the tight SVX selection. QCD is the latter number divided by the efficiency of the tight SVX requirements. Ghost is the difference between the total and the QCD contributions.

Topology	Total	SVX	QCD	Ghost
$N_c \geq 0$	1426571	275986	1131090 ± 9271	295481 ± 9271
$N_c \geq 1$	141039	22981	94184 ± 772	46855 ± 772
OS	94148	15372	63000 ± 516	31148 ± 516
SS	57106	8437	34578 ± 283	22528 ± 283
$N_c \geq 2$	10215	828	3393 ± 28	6822 ± 28

TABLE V: Numbers and types of three-muon combinations. We separate events according to the charge of the initial muons. The topology OSO is that of two opposite-charge initial dimuons; by definition, the third muon has opposite charge with respect to one of them. When initial dimuons have same sign charge, the third muon charge can have either the same (SSS) or opposite sign (SSO).

Topology	All	SVX	QCD	Ghost
OSO	90022	14497	59414 ± 487	30608 ± 487
SSO	48220	7708	31590 ± 259	16630 ± 259
SSS	28239	4139	16963 ± 139	11276 ± 139

the ghost contribution is the difference between the data and the QCD contribution. The number of three-muon combinations is listed in Table V. Figure 18 shows the invariant mass and opening angle distribution of OSO combinations for the QCD and ghost contributions. Muon pairs due to b sequential decays, that provide most of the QCD contribution, peak at small invariant masses and small opening angles. The tail at large masses and opening angles

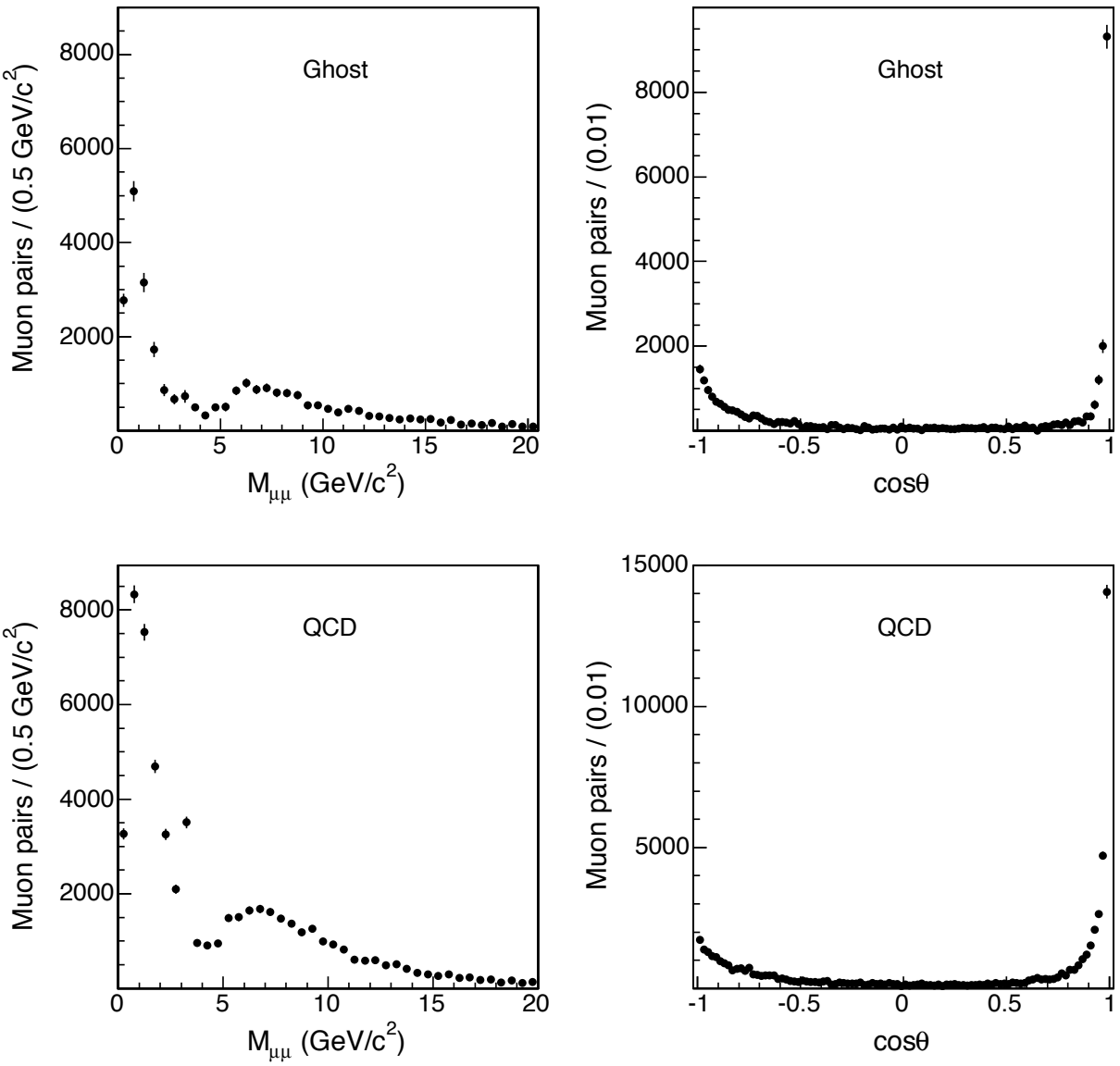

FIG. 18: Events with OS initial muon pairs and an additional muon that is combined with the opposite charge initial muon. We plot the invariant mass, $M_{\mu\mu}$, and opening angle, θ, distributions of these combinations for the QCD and ghost contributions.

results from fake muons with wrong charge. The distributions of analogous pairs due to the unexpected background have a quite similar behaviour. However, it is important to note that combinations of initial and additional muons in ghost events have a smaller opening angle than those from sequential b decays. As shown in Fig. 19, SSO and SSS combinations have similar opening angle distributions. It seems therefore reasonable to restrict the study of ghost events to muons and tracks contained in a cone of angle $\theta \leq 36.8^{\circ}$ around the

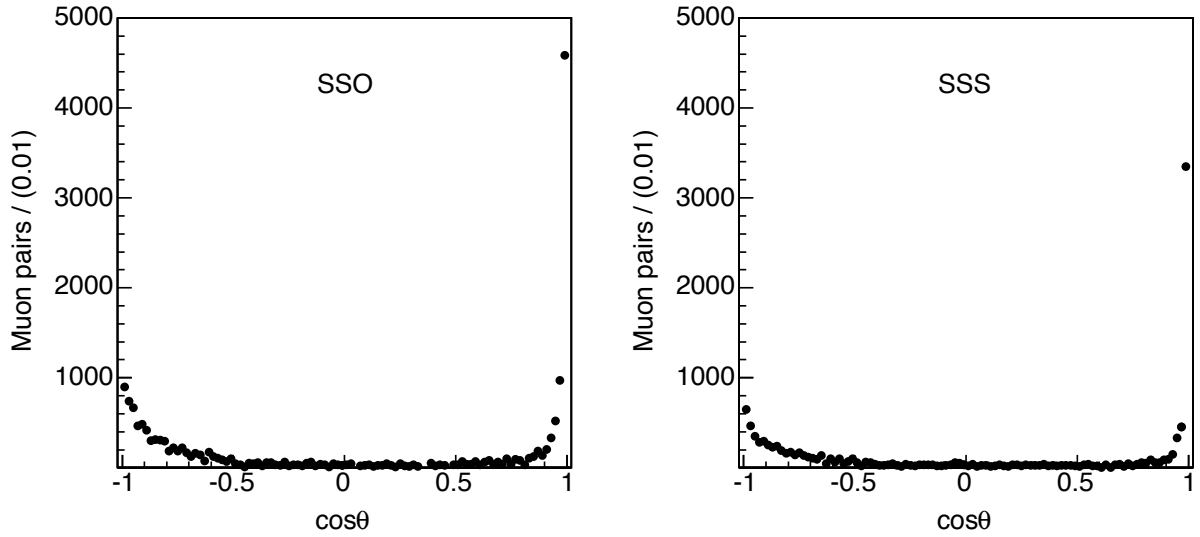

FIG. 19: Opening angle distributions of dimuon combinations for events due to the unexpected background. The initial dimuons have same sign charge, and combinations of an additional and initial muons are split according to the charge of the additional muon. The plots are the projection of two-dimensional distributions in which the additional muon is combined with both initial muons.

TABLE VI: Numbers of additional muons with an angle $\theta \leq 36.8^{\circ}$ with respect to the direction of one of the initial muons. We list separately the combination of additional and initial muons with opposite (OS) and same (SS) sign charge.

Topology	All	SVX	QCD	Ghost
OS	83237	13309	54545 ± 447	28692 ± 447
SS	50233	7333	30053 ± 246	20180 ± 246

direction of each initial muon.

VI. STUDY OF MUON AND TRACK PROPERTIES IN GHOST EVENTS

The number of additional muons that are contained in a cone of angle $\theta \leq 36.8^{\circ}$ ($\cos\theta \geq 0.8$) around the direction of any initial muon is listed in Table VI. Figure 20 shows the two-dimensional distribution of the impact parameter of an initial muon versus that of all additional muons in a $\cos\theta \geq 0.8$ cone around its direction. The QCD contribution has

TABLE VII: Numbers of tracks with $p_T \geq 2$ GeV/c, $|\eta| \leq 1.1$, and an angle $\theta \leq 36.8^\circ$ with respect to the direction of one of the initial muons. We list separately the number of tracks with opposite (OS) and same (SS) charge as the initial muon. We do not consider tracks that are associated with a muon stub.

Topology	All	SVX	QCD	Ghost
OS	1315451	207344	849770 ± 6965	465860 ± 6965
SS	893750	140238	574745 ± 4711	318004 ± 4711

been removed using events in which the primary muons pass the tight SVX requirement. The tail of the impact parameter distribution of additional muons in QCD events, shown in Fig. 21, does not extend beyond 2 mm. In contrast, as shown in Fig. 20, the impact parameter distribution of additional muons in ghost events extends to much larger values and is consistent with that of initial muons. However, the impact parameter of the additional and initial muons are not very correlated (the correlation factor is $\rho_{d_p d_s} = 0.03$). A correlation factor of this size is typical of uncorrelated muon pairs arising from semileptonic decays of different b- or c-quarks.

The contribution of fake muons is evaluated by weighting all tracks with $p_T \geq 2$ GeV/c, $|\eta| \leq 1.1$, and contained in a $\cos\theta \geq 0.8$ cone, with the fake probabilities shown in Fig. 14. Table VII lists the number of these tracks for QCD and ghost events. The QCD and ghost contributions have been previously determined to be 1131090 and 295481 events, respectively. It follows that the average number of tracks contained in a $\theta \leq 36.8^\circ$ cone around the direction of one of the initial muons due to ghost events is 1.58 OS and 1.08 SS, a factor of two higher than that of QCD events (0.75 OS and 0.51 SS tracks).

Table VIII compares the observed number of additional muons to the predicted number of additional fake muons in ghost events. In ghost events, the fraction of real muons, with opposite or same charge, is approximately four times larger than that of real muons in QCD events (9.4% versus 2.1%, as obtained from the number of $OS - SS$ dimuons listed in Table VI and the number of $OS + SS$ dimuons in ghost events after subtracting the average of the pion and kaon fake contributions listed in Table VIII, respectively). In Table VIII, the ratio of real to background muons is approximately 1/1. This ratio is larger than that

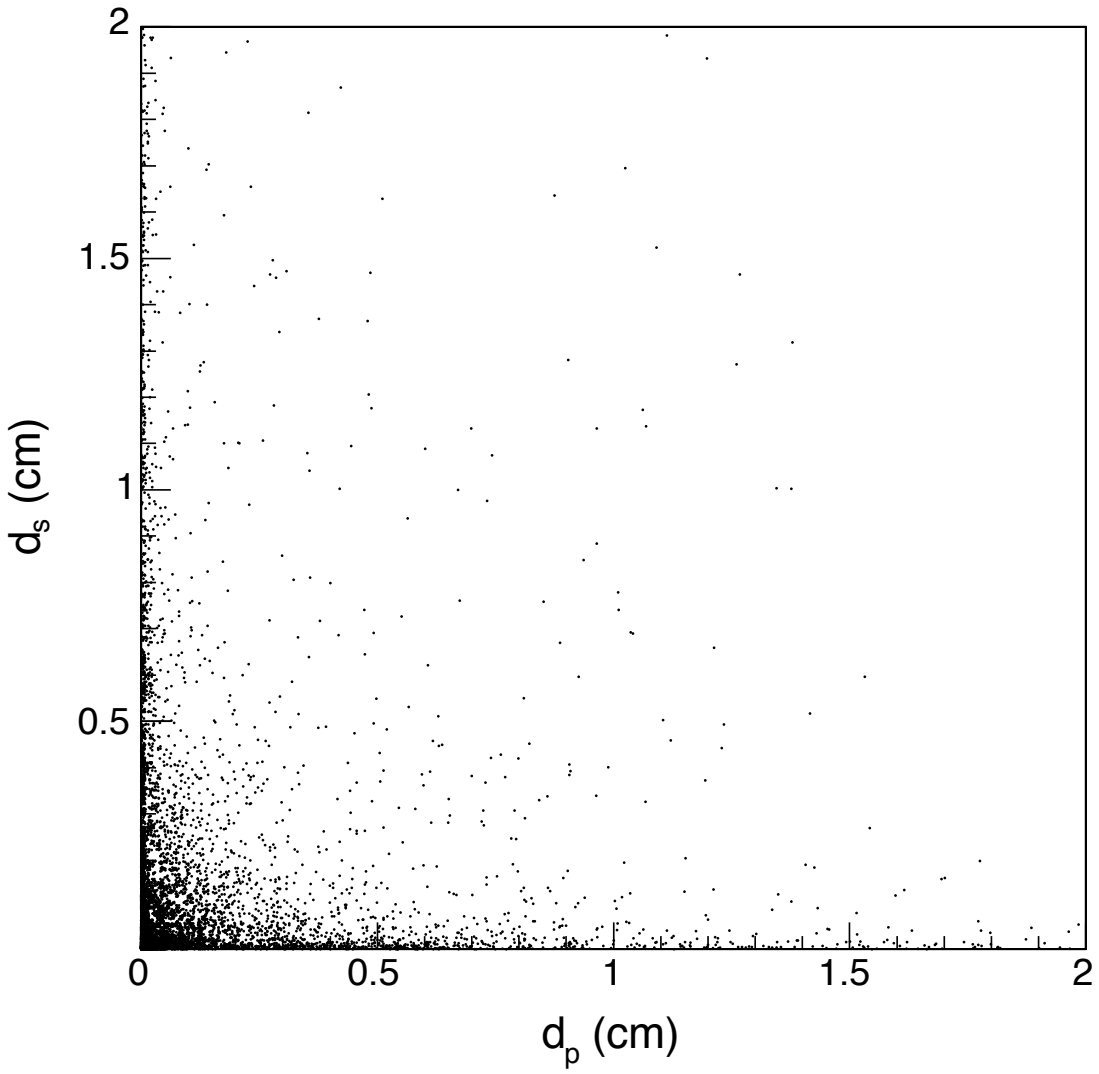

FIG. 20: Two-dimensional distribution of the impact parameter of an initial muon, d_p, versus that, d_s, of additional muons for the unexpected background. Muons are selected with loose SVX requirements. The QCD contribution has been removed.

in QCD events, 1/2.5, that are correctly modeled by the heavy flavor simulation. However, because ghost events appear anomalous, we want to verify the estimate of the fraction of additional real muons by selecting CMUP muons with $p_T \geq 3$ GeV/c. In this case, the contribution of fake muons, calculated as in Ref. [6], is expected to be negligible. The numbers of additional CMUP muons and expected fakes are listed in Table IX. One notes that the fake contribution is much reduced, however at the expense of the muon acceptance

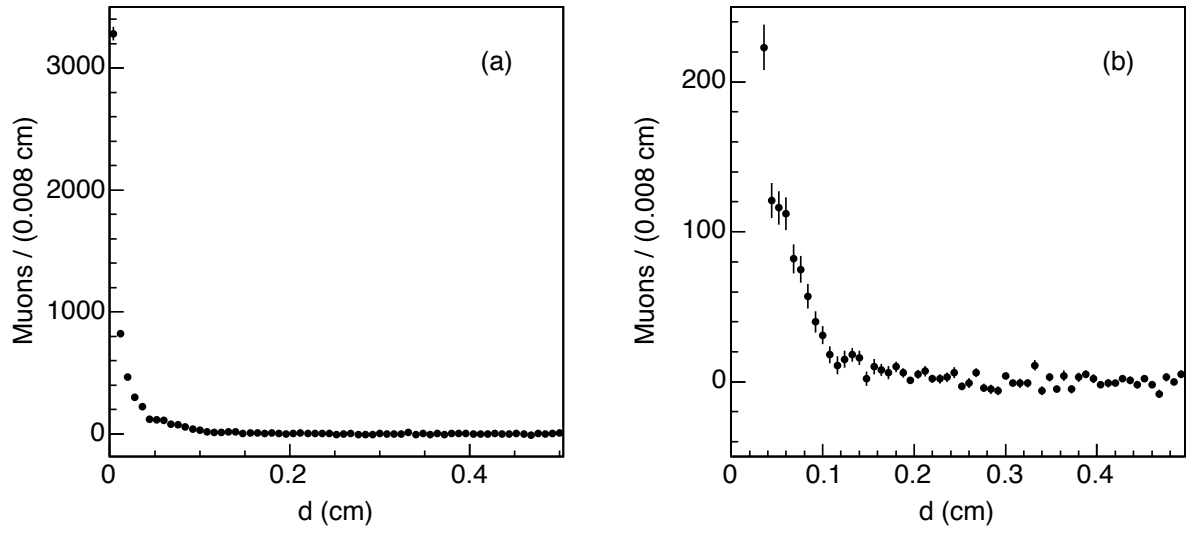

FIG. 21: Impact parameter distribution of (a) additional muons found in QCD events. The same distribution (a) is plotted with an expanded vertical scale. Additional muons are selected without SVX requirements.

TABLE VIII: Numbers of additional muons in ghost events are compared to fake muon expectations. The fake muon prediction is evaluated applying the fake probabilities shown in Fig. 14 to all tracks not associated to a muon stub and with $p_T \geq 2$ GeV/c, $|\eta| \leq 1.1$, and an angle $\theta \leq 36.8^{\circ}$ with respect to the direction of one of the initial muons. We list separately the number of muons with opposite (OS) and same (SS) sign charge as the initial muon. F_K and F_π are the number of fake muons predicted assuming that hadronic tracks are all kaons or all pions, respectively. For kaon tracks, the rate of predicted fake muons should by increased by 10% to also account for in-flight-decay contributions.

Topology	Observed	F_K	F_π
OS	28692 ± 447	15447 ± 210	9649 ± 131
SS	20180 ± 246	10282 ± 137	6427 ± 81

that decreases by a factor of approximately five. The fraction of real CMUP muons is $(0.40 \pm 0.01)\%$ in QCD events, and is four times larger $(1.64 \pm 0.08)\%$ in ghost events. This result is consistent with the previous determination that uses all muon detectors.

TABLE IX: Numbers of additional CMUP muons in QCD and ghost events. F_π are the numbers of fake muons in ghost events, predicted assuming that hadronic tracks are pions. In QCD events, the fake contribution is the number of SS combination.

Topology	All	QCD	Ghost	F_π
OS	10812	7380 ± 172	3432 ± 201	216 ± 44
SS	4400	2635 ± 104	1765 ± 123	138 ± 35

One concludes that ghost events are indeed quite interesting because a $\cos\theta \geq 0.8$ cone around the direction of a primary muon contains twice as many tracks than QCD events. In addition, these cones contain a fraction of real muons that is approximately four times larger than that of QCD events. Additional and initial muons have both anomalously large impact parameters that are not strongly correlated. Since at least 40% of this unexpected background is accounted for by ordinary SM contributions, the remaining fraction of ghost events contains a surprisingly large number of tracks and muons with $p_T \geq 2$ GeV/c per event.

Figure 22 (a) shows the distribution of the number of muons found in a $\cos\theta \geq 0.8$ cone around a primary muon due to ghost events. In the plot, an additional muon increases the multiplicity by 1 when of opposite and by 10 when of same sign charge as the initial muon. It is an obvious observation that a small fractions of ghost events contain a very large muon multiplicity. The contribution of fake muons is estimated assuming that the large majority of the tracks in a $\cos\theta \geq 0.8$ cone are pions. We correct the distribution in Fig. 22 (a) as follows. Given an event with n muons, we loop over the tracks not associated to a muon stub and with the same kinematic properties of muon candidates and randomly generate fake muons using the probability that a pion mimics a muon signal. If m is the number of generated fake muons, we remove one event with $m + n$ muons in the distribution in Fig. 22 (a) and add one event to the bin with n muons. The resulting distribution is shown in Fig. 22 (b). The number of cases in which a $\cos\theta \geq 0.8$ cone around the direction of a primary muon contains one or more additional muons is reduced from 40409 to 27539.

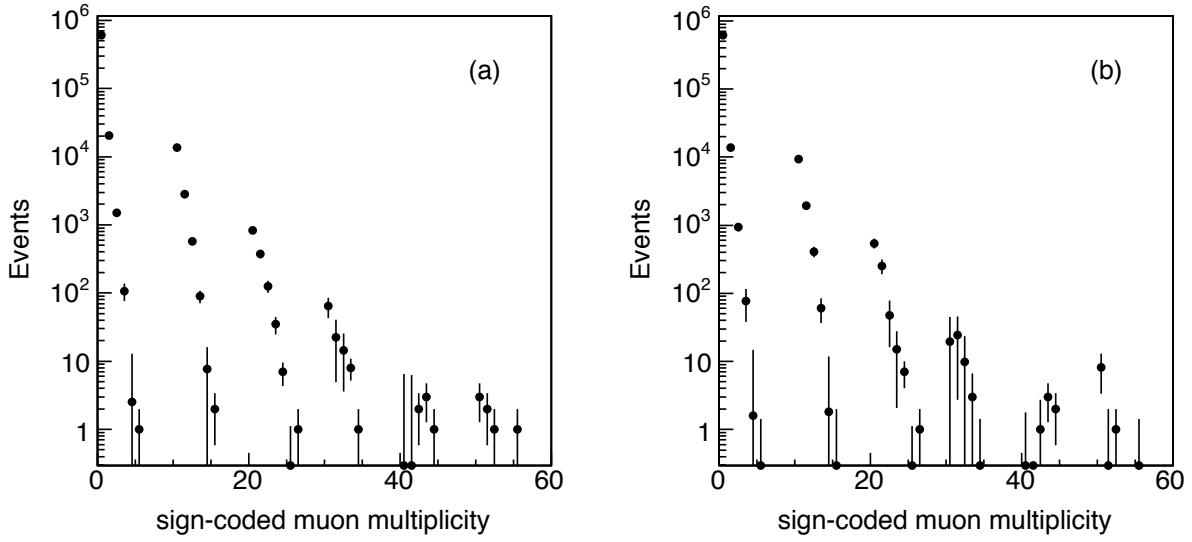

FIG. 22: Sign-coded multiplicity distribution of additional muons found in a $\cos\theta \geq 0.8$ cone around the direction of a primary muon in ghost events before (a) and after (b) correcting for the fake muon contribution. An additional muon increases the multiplicity by 1 when has opposite and by 10 when has same sign charge as the initial muon. The background subtracted distribution is also listed in Table X.

A. Robustness of the fake muon prediction

Given the anomaly of the observation, it seems important to further verify that such a large number of muons contained in such a small angular cone is not a detector artifact. A visual inspection of events that contain four or more muons did not yield any indication of a detector malfunction. However, there are events in which certain areas of the muon detectors have a dense clustering of dozens of hits. In these events, some muons correspond to tracks linked to muon stubs constructed in those clusters. We estimate the muon fake rate using the probability that pions and kaons from D^0 decays mimic a muon signal. Even if we require that D^0 candidates have an appreciable proper decay time in order to select D^0 mesons from b-hadron decays, a 36.8° cone around the direction of these tracks contains an average of 0.02 muons and 1.6 additional tracks with $p_T \geq 2$ GeV/c. The muon fake probability does not increase at all when using D^0 prongs accompanied by at least two tracks. However, the multiplicity in a 36.8° cone around the direction of the D^0 prongs does not have the high multiplicity tail of ghost events, and one worries that our procedure might underestimate

TABLE X: Sign-coded, background subtracted, muon multiplicity in ghost events. Bins without entries are not shown. The multiplicity is not acceptance corrected because we do not know the mechanism producing ghost events. However, the detector acceptance for an additional muon with $p_T \geq 2$ GeV/c and $|\eta| \leq 1.1$ is 0.838 ± 0.004. The detector acceptance for an initial muon with $p_T \geq 3$ GeV/c and $|\eta| \leq 0.7$ is 0.506 ± 0.003.

Bin	Content	Bin	Content
0	620307.31 ± 3413.55	30	19.43 ± 25.64
1	13880.17 ± 572.94	31	24.22 ± 21.47
2	941.50 ± 134.83	32	9.80 ± 13.80
3	77.24 ± 39.23	33	3.00 ± 3.61
4	1.61 ± 13.20	34	0.00 ± 1.41
5	0.00 ± 1.41	40	-7.39 ± 9.17
10	9312.12 ± 425.01	41	-7.20 ± 6.97
11	1938.23 ± 173.48	42	1.00 ± 1.73
12	409.10 ± 71.48	43	3.00 ± 1.73
13	60.31 ± 23.45	44	2.00 ± 1.41
14	1.80 ± 10.06	50	8.10 ± 4.77
15	0.00 ± 2.00	51	0.00 ± 2.00
20	542.38 ± 90.76	52	1.00 ± 1.00
21	250.85 ± 61.25	53	0 ± 0
22	47.04 ± 30.91	54	0 ± 0
23	14.90 ± 12.84	55	0.00 ± 1.41
24	7.00 ± 3.00		
25	-3.10 ± 4.22		
26	1.00 ± 1.00		

the fake rate in multi-muon events in which hadronic tracks can take advantage of hits in the muon chambers produced by real muons or by hadronic punchthrough. Our muon selection criteria are quite benign and certainly were not tuned for this type of dramatic events. A

track is accepted as a muon if the distance of its projection onto a muon detector from a muon stub is $\Delta x \leq 30$, 40, and 30 cm for the CMU, CMP, and CMX detector, respectively. For a muon with $p_T = 2$ GeV/c, these Δx cuts correspond to the requirement that the track extrapolation and the muon stub match within 3 σ in the $r - \phi$ plane, where σ is a standard deviation that includes the effect of multiple scattering and energy loss. We have selected additional muons by adding the increasingly stricter requirements that track-stub matches are within 3 and 2 σ, respectively. The latter requirement reduces the number of multiple-muon combinations by a factor of two, but does not affect the salient features of the multiplicity distribution in Fig. 22 (a). We have compared Δx and σ distributions of muon-track matches for the different muon detectors in QCD and ghost events. These distributions, as well as the fractional usage of different muon detectors, in ghost events are not different to those of QCD events. Since we are able to predict the rate of additional muons in QCD events, which have a larger fake muon background than ghost events, the estimate of the fake muon background cannot provide the explanation for the large excess of additional muons in ghost events. We have also verified one extreme hypothesis. Traditionally, searches for soft ($p_T \geq 2$ GeV/c) muons performed by the CDF collaboration estimate the fake muon contribution by using a fake probability per track [25]. If the excess of muons in ghost events were due to a breakdown of this method when applied to high E_T jets with many tracks that are not contained in the calorimeter and muon absorber, we should also have observed the presence of multi-muons events in QCD data. This effect has never been observed in previous analyses, and, as shown in Fig. 23, the distributions of the transverse momentum carried by all tracks with $p_T \geq 1$ GeV/c contained in a 36.8° around an initial muon are quite similar in ghost and QCD events. The appearance of multi-muons seems to be correlated with the presence of muons with large impact parameters. As discussed earlier, secondary interactions in the detector volume do not contribute significantly to the total number of ghost events. This does not exclude the possibility that the smaller number of multi-muon events that cannot be accounted for by the SM sources of ghost events are due to secondary interactions in the detector volume that point into calorimetry cracks. We search for secondary interactions by combining initial muons with small and large impact parameter with all additional muons in a 36.8° cone around the muon direction. Dimuon combinations are constrained to arise from a common space point. They are discarded if the three-dimensional vertex fit returns a χ^2 per degree of freedom larger than 10. The

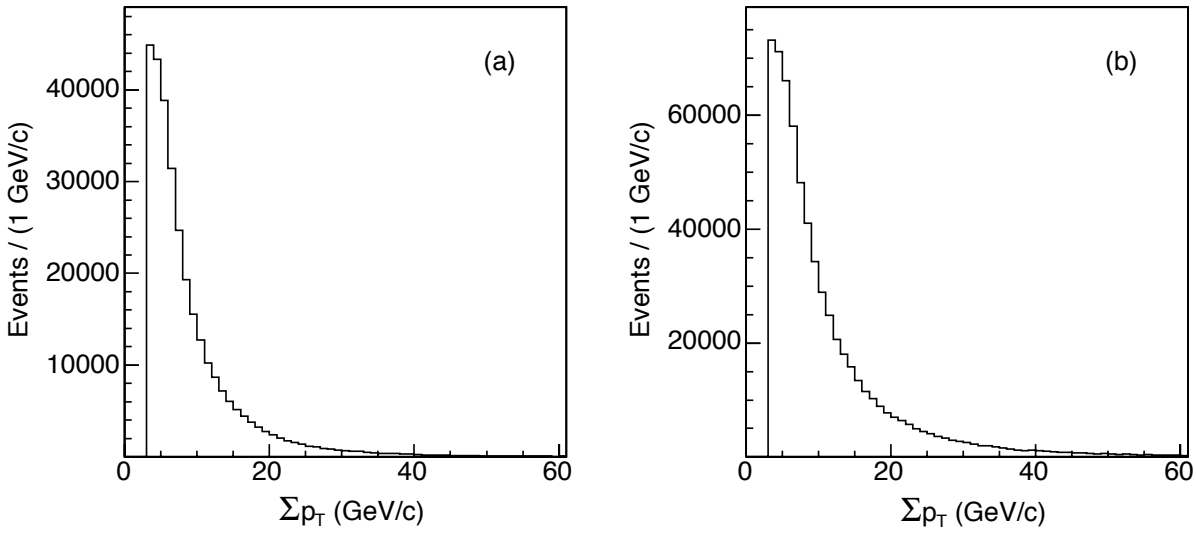

FIG. 23: Distribution of the transverse momentum carried by all tracks with $p_T \geq 1$ GeV/c contained in a 36.8° around an initial muon in (a) QCD and (b) ghost events.

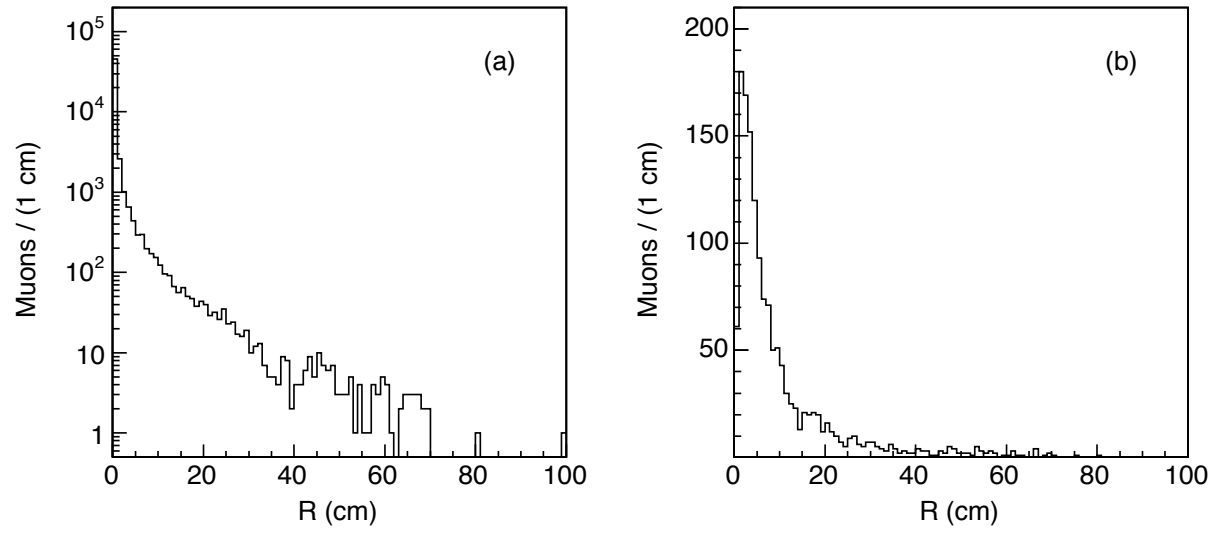

FIG. 24: Distributions of R, the distance of dimuon vertices from the nominal beam line for initial muons with impact parameter (a) smaller and (b) larger than 0.3 cm.

distribution of R, the distance of a reconstructed secondary vertex from the detector origin in the plane transverse to the beam line, is shown in Fig. 24 for initial muons with small and large impact parameters. The absence of spikes in the distribution does not support the possibility that secondary interactions are the cause of multi-muon events.

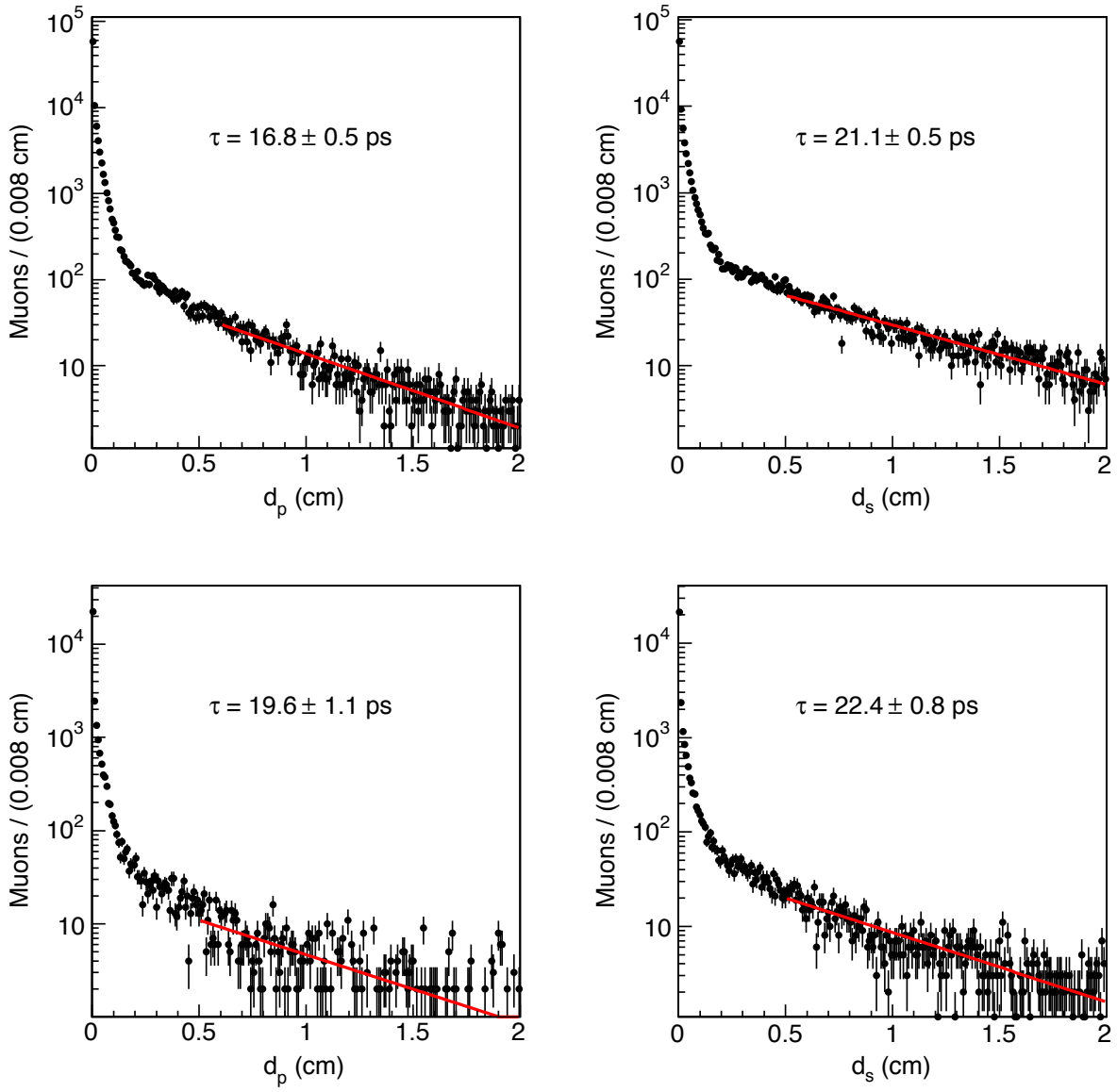

FIG. 25: Muon impact parameter distributions for events containing (top) only two muons or (bottom) more than two muons in a $\cos\theta \geq 0.8$ cone. We call d_p and d_s the impact parameter of initial and additional muons, respectively. The solid lines represents fits to the data distribution with an exponential function. The fit result is shown in each plot.

VII. INVESTIGATION OF ADDITIONAL PROPERTIES OF MULTI-MUON EVENTS

We verify again the muon impact parameter distributions for the subset of ghost events in which a cone contains two or more muons. The impact parameter distribution of initial

muons due to ghost events in Fig. 6 is derived using muon tracks that pass the loose SVX selection in order to minimize the possible contribution of interactions in the detector systems surrounding the SVXII detector. As mentioned earlier, this requirement sculpts the impact parameter distribution of muons arising from the decay of particles with a lifetime much larger than that of b quarks. The smaller number of events that contain two or more muons in a $\cos\theta \geq 0.8$ cone is not contaminated by secondary interaction, and we select muons without any SVX requirement. The corresponding impact parameter distributions are shown in Fig. 25. Fits with an exponential function to the impact parameter distributions of additional muons in the range $0.5-2.0$ cm return a lifetime of approximately 21.4 ± 0.5 ps. One notes that the fits to the impact parameters of initial muons yield smaller values of the lifetime. The difference is understood in term of kinematic and trigger biases affecting the initial muons. As an example, Fig. 26 compares the result of fits to the impact parameter of muons and tracks corresponding to identified K^0_S decays. One notes that the fit to the track impact parameter yields a K^0_S lifetime in agreement with PDG value of $c\tau = 2.468$ cm. In contrast, the lifetime measurement using the initial muons yields a much smaller lifetime value, similar to that of the initial muons in ghost events. The lifetime returned by the fits to the additional muons is intriguing since no known particle has a lifetime of this order of magnitude. The fact that multi-muon events appears when the trigger muons are requested to originate outside the beam pipe implies that they are produced by objects with a lifetime much larger than that of b quarks. However, this lifetime measurement is based on a small fraction of events in the tail of the impact parameter distribution, and one could be mislead by kinematic biases affecting small SM backgrounds that might survive the multi-muon request.

Conversely, one might wonder if the impact parameter tail is a detector effect that has been ignored in all studies of t- and b-quark physics performed by the CDF collaboration. These analyses customarily utilize muons and tracks with impact parameters smaller than $0.1-0.2$ cm. Figure 27 plots impact parameter distributions of CMUP muons accompanying a $D^0 \rightarrow \pi^+K^-$ and charge conjugate candidate. We use events acquired with the μ-SVT trigger and reconstruct D^0 candidates by attributing the kaon mass to the track with the same charge as the muon (RS combinations as expected for $\mu + D^0$ systems produced by B hadron decays). We retain combinations in which the muon plus di-track system has invariant mass smaller than 5 GeV/c^2.No wrong-sign (WS) combinations are found. We

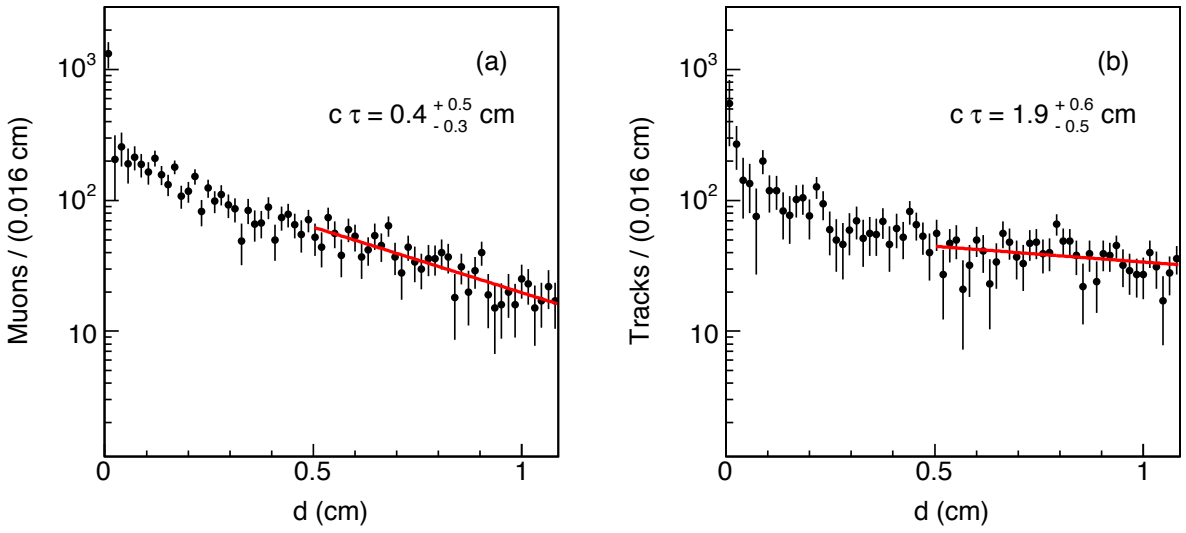

FIG. 26: Impact parameter distributions of (a) initial muons and (b) tracks of identified K^0_S decays. The combinatorial background under the K^0_S signal in Fig. 10 has been removed using a sideband subtraction method.

use a sideband subtraction method to remove the combinatorial background in the invariant mass region corresponding to the D^0 signal. One concludes that the tail at large impact parameters for initial trigger muons in ghost events is not a detector effect. Figure 28 is the analogous plot when muons are selected as the additional muons in this analysis ($p_T \geq 2$ GeV/c and $|\eta| \leq 1.1$). No high impact parameter tails are observed. The fraction of fake muons, measured as the number of WS combinations, is approximately 2%.

A. Track multiplicity

As discussed in Sec. VI, ghost events include a sizable contribution of SM sources such as in-flight-decays, K^0_S, and hyperon decays. The average track multiplicity in ghost events is a factor of two larger than QCD events. In order to study the average multiplicity of multi-muon events, we use events that contain at least three muons in a 36.8° cone. Figure 29 shows the average number of all tracks with $p_T \geq 2$ GeV/c contained in a 36.8° cone around a primary muon as a function of the total transverse momentum of the tracks.

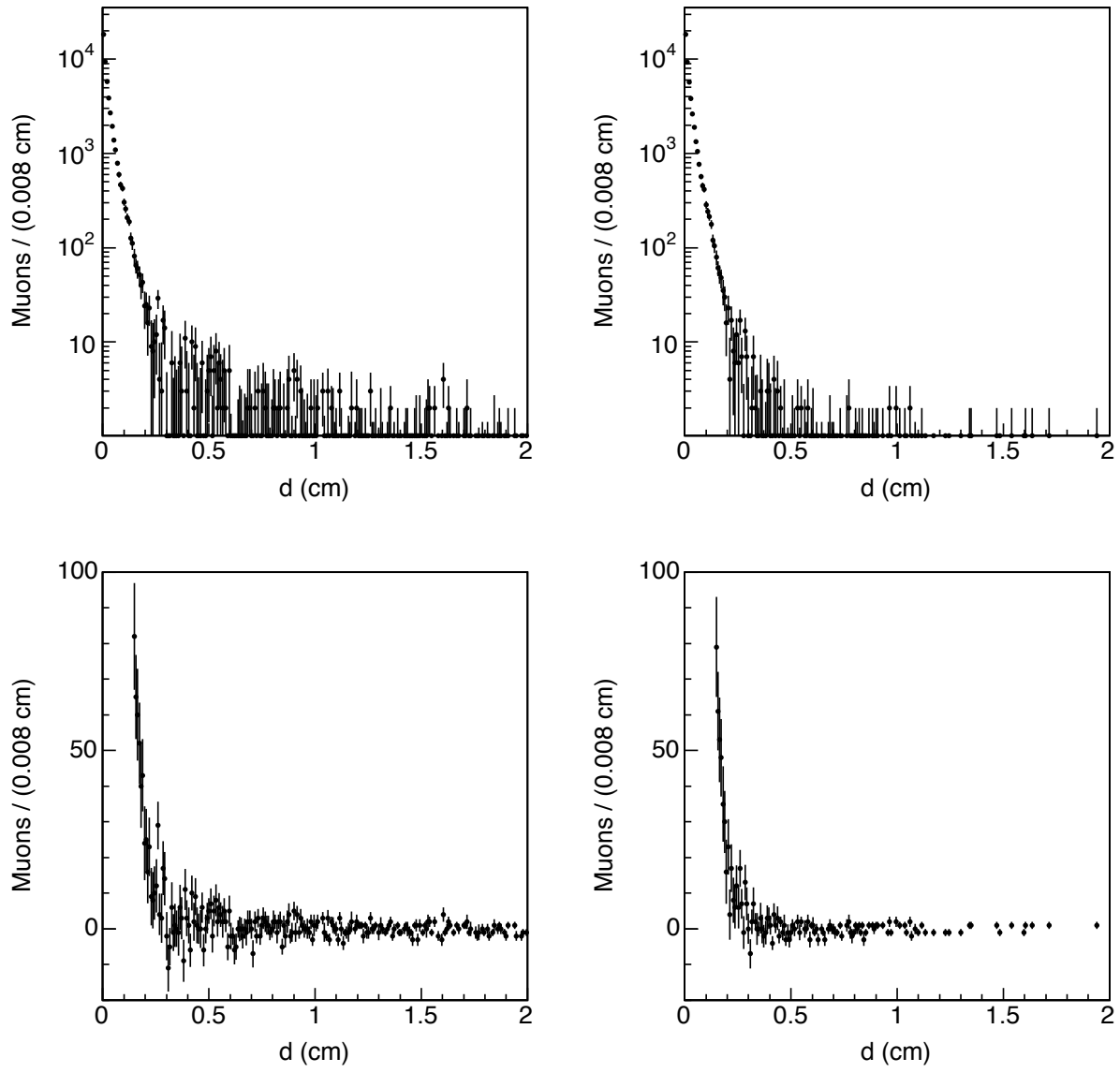

FIG. 27: Impact parameter distributions of CMUP muons which are accompanied by a D^0 meson and are selected without (left) SVX requirements or with (right) loose SVX requirements. The bottom plots are exploded views that show distributions at large impact parameters. The contribution of the combinatorial background under the D^0 signal has been removed with a side-band subtraction method.

B. Cone correlations

In the previous section, we have investigated the kinematics and topology of muons and tracks contained in a single 36.8° cone around the direction of an initial muon. In this

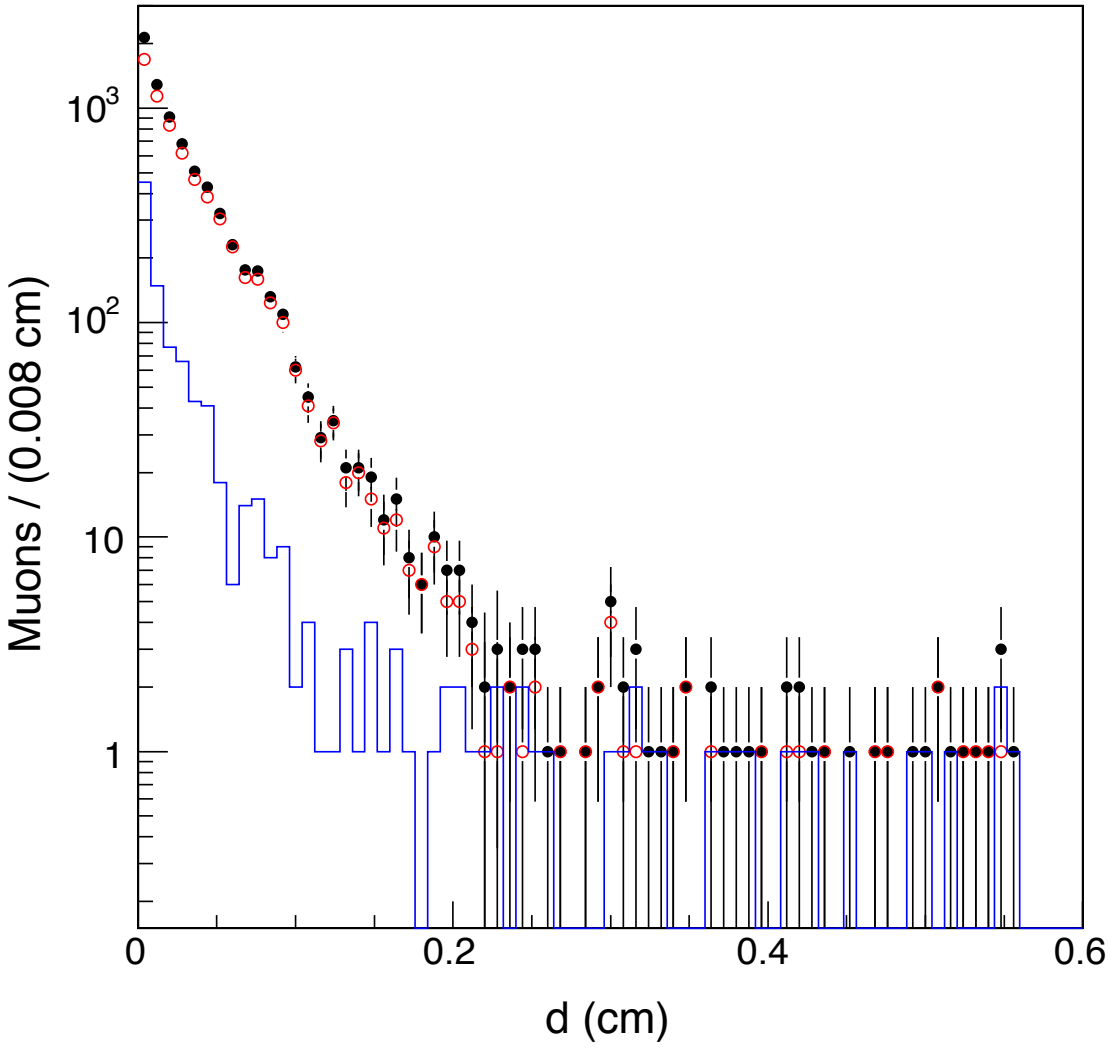

FIG. 28: Impact parameter distributions of muons accompanied by a D^0 meson and selected as the additional muons in this analysis. No SVX requirements are applied. All events (•) are compared to RS (○) and WS (histogram) combinations (see text). The contribution of the combinatorial background under the D^0 signal has been removed with a side-band subtraction method.

section, we extend the investigation to the rate and properties of events in which two 36.8° cones contain a muon multiplicity larger than that of QCD events. After subtracting the QCD and fake muon contribution, in events due to the unexpected background there are 27990 ± 761 cones that contain two or more muons, 4133 ± 263 cones that contain three or more muons, and 3016 ± 60 events in which both cones contain two or more muons.

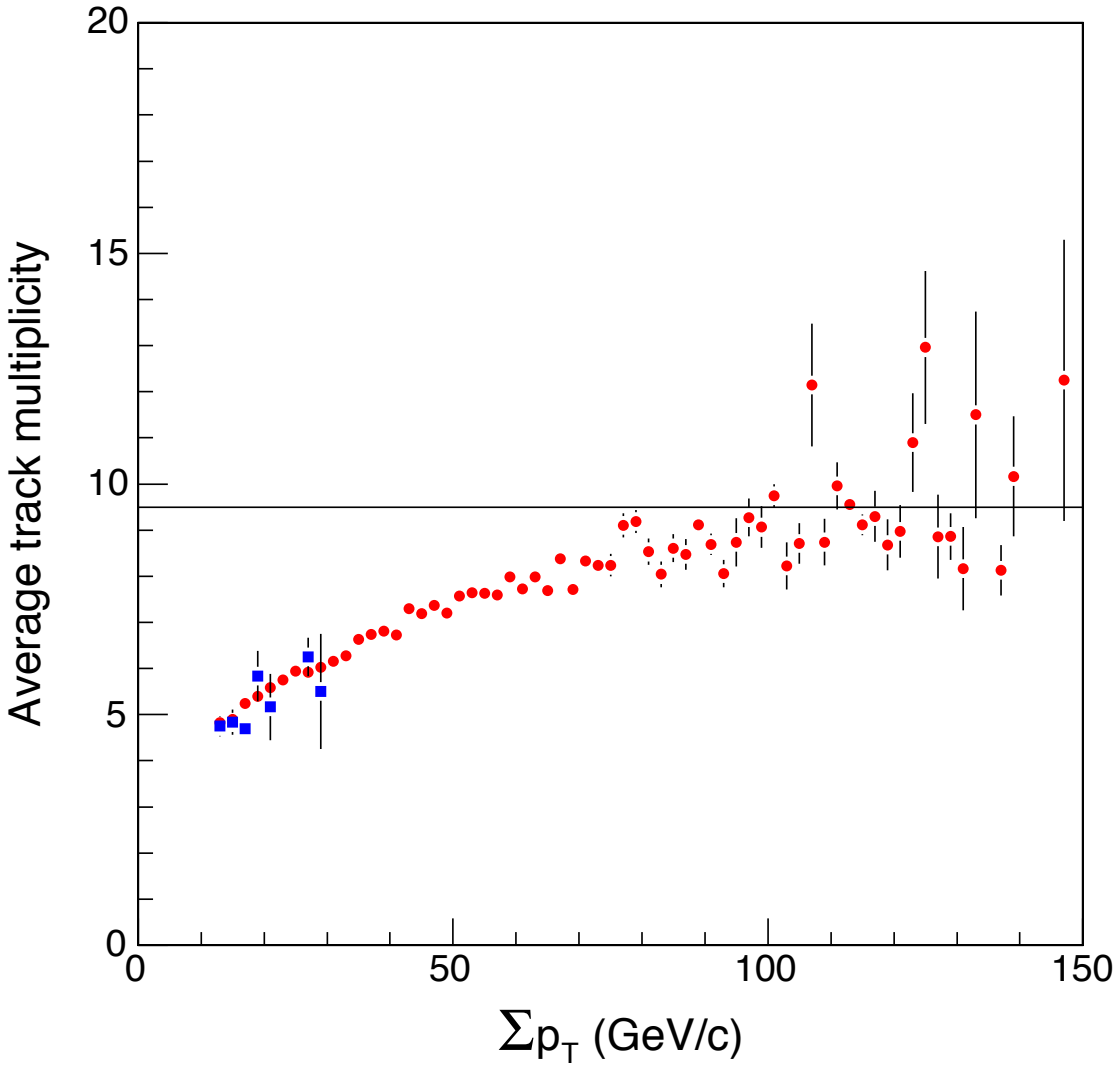

FIG. 29: Average number of tracks in a 36.8° cone around the direction of a primary muon as a function of $\sum p_T$, the transverse momentum carried by all the tracks. We use cones containing at least three muons. Data (•) are compared to the QCD expectation (■) based on the few events predicted by the heavy flavor simulation, normalized to the number of initial dimuons in the data and implemented with the probability that hadronic tracks mimic a muon signal. The detector efficiency for these tracks is close to unity.

It follows that approximately 13% of the ghost events in which one cone contains two or more muons also contain a second cone with the same characteristics. In events triggered by a central jet, the fraction of events also containing an additional central jet is $10 - 15\%$

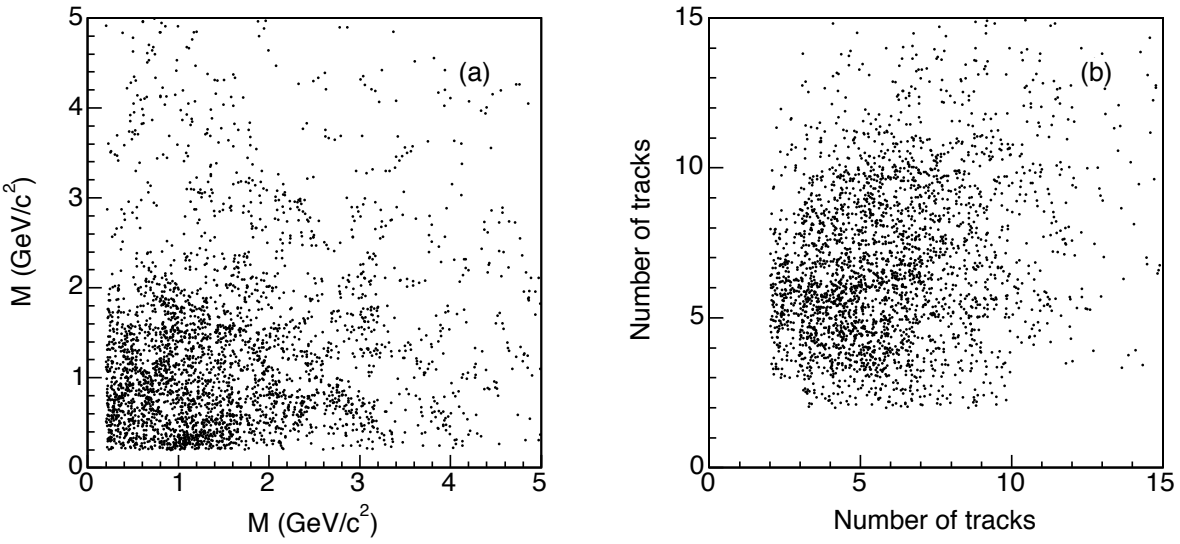

FIG. 30: Two-dimensional distributions of (a) the invariant mass, M, of all muons and (b) the total number of tracks contained in a 36.8° cone when both cones contain at least two muons. The QCD and fake muon contributions have been subtracted.

depending on the jet transverse energy [28]. The observed fraction of ghost events with two multi-muon cones makes it difficult to think of detector effects that might produce this type of events. For example, if these events were due to punchthrough of high E_T jets, that for not-yet-understood reasons do not show up in QCD events, we would observe either a very small fraction of events with two multi-muon cones or an incredibly larger number of events with single multi-muon cones.

Figure 30 plots two-dimensional distributions of the invariant mass of all muons and of the number of tracks with $p_T \geq 2$ GeV/c contained in each cone for the 3016 events. Figure 31 shows that the invariant mass distribution of all muons contained in the 27990 cones containing at least two muons is consistent with that of the 3016 events in which both cones contain at least two muons. Figure 32 shows the invariant mass distribution of all muons and all tracks with $p_T \geq 2$ GeV/c in events in which both cones contains two or more muons.

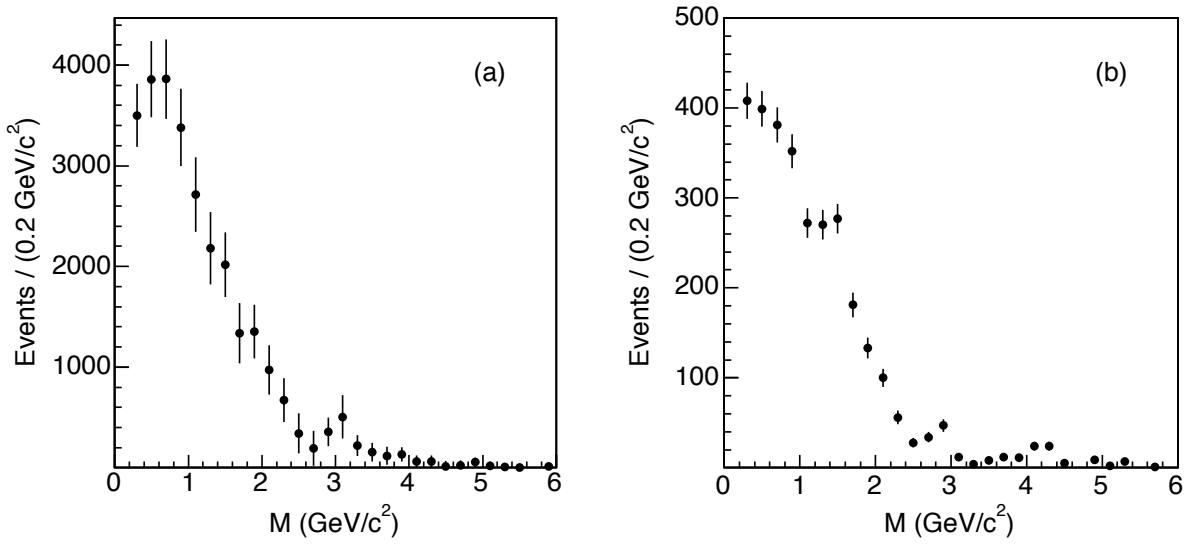

FIG. 31: Distributions of invariant mass, M, of all muons contained in (a) the 27990 36.8° cones with two or more muons and (b) the 3016 events in which both cones contain two or more muons.The QCD and fake muon contributions have been subtracted.

VIII. CONCLUSIONS

We have studied a sample of events containing at least two central muons with $p_T \geq 3$ GeV/c and invariant mass larger than 5 GeV/c^2. The data set was collected with the CDF II detector at the Fermilab Tevatron collider, and corresponds to an integrated luminosity of 2100 pb^{-1}. Similar data sets have been previously used by the CDF and DØ collaborations to derive measurements of the correlated $\sigma_{b\to\mu,\bar{b}\to\mu}$ cross section that do not agree among themselves. A similar data set was used by the CDF collaboration to extract a value of $\bar{\chi}$, the average time-integrated mixing probability of b-flavored hadrons, that is appreciably larger than that reported by the LEP experiments. This analysis extends a recent study [6] by the CDF collaboration which has used a dimuon data sample to re-measure the correlated $\sigma_{b\to\mu,\bar{b}\to\mu}$ cross section. In Ref. [6], the value of $\sigma_{b\to\mu,\bar{b}\to\mu}$ is determined by fitting the impact parameter distribution of these primary muons with the expected shapes from all known sources. The data are nicely described by a fit with contributions from the following QCD processes: semileptonic heavy flavor decays, prompt quarkonia decays, Drell-Yan production, and instrumental backgrounds from hadrons mimicking the muon signal. Using the fit result, Ref. [6] reports $\sigma_{b\to\mu,\bar{b}\to\mu} = 1549 \pm 133$ pb for muons with $p_T \geq 3$ GeV/c and

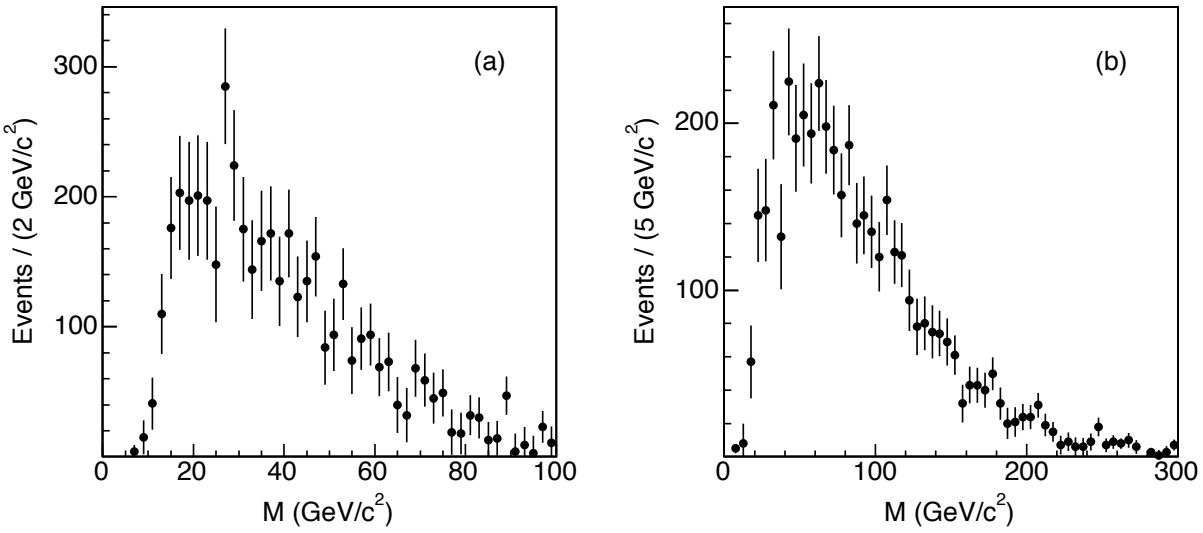

FIG. 32: Invariant mass distribution of (a) all muons and (b) all tracks for events in which both cones contain at least two muons. The QCD and fake muon contributions are subtracted. The data correspond to an integrated luminosity of 2100 pb^{-1}.

$|\eta| \leq 0.7$. That result is in good agreement with theoretical expectations as well as with analogous measurements that identify b quarks via secondary vertex identification [26, 27]. To ensure an accurate impact parameter determination, Ref. [6] uses a subset of dimuon events in which each muon track is reconstructed in the SVX with hits in the two inner layers and in at least four of the inner six layers. The tight SVX requirements select events in which both muons arise from parent particles that have decayed within 1.5 cm from the nominal beam line. According to the simulation, approximately 96% of the dimuon events contributed by known QCD processes satisfy this condition. The present study tracks the origin of these inconsistencies to background events, referred to as ghosts, in which at least one of the trigger muons is produced on the outside of the beam pipe, that are rejected differently by different SVX requirements. The magnitude of this background contribution is comparable to the $b\bar{b}$ contribution when no SVX selection is made and in combination would account for the measurement reported in [8]. Similarly, for the loose SVX criteria, the magnitude of the ghost contribution, when added to the expected $b\bar{b}$ contribution, coincides with the cross section measurement reported in [7] and the $\bar{\chi}$ value reported in [4] since these measurements use similar sets of silicon criteria. Moreover, when applying the tight SVX criteria to initial muons, the invariant mass spectrum of combinations of an initial

muon with an additional accompanying muon is well described by known QCD sources and is dominated by sequential semileptonic heavy flavor decays. In contrast, without any SVX requirement the invariant mass spectrum cannot be modeled with the SM simulation and the inconsistencies at low invariant mass reported in [3] are reproduced. Thus, this source of dimuon events seems to offer a plausible resolution to these long-standing inconsistencies related to $b\bar{b}$ production and decay. A large portion of these events is due to muons arising from in-flight-decays of pions and kaons or punchthrough of hadronic prongs of K^0_S and hyperon decays. However, a small fraction of this background contains muons that appear to originate from the decay of particles with a lifetime an order of magnitude longer than that of b quarks. Ghost events have additional properties that are markedly different from those of QCD events. An angular cone of 36.8° around the direction of an initial muon contains a rate of additional muons ($\simeq 15\%$) that is larger than that produced by cascade semileptonic decays of b quarks. In contrast with sequential semileptonic decays of b hadrons, additional muons can have a charge the same or opposite as that of the initial muons with equal probability. After removing the contributions of muons mimicked by hadronic tracks, a 36.8° cone contains muon multiplicities as large as 8. The average number of tracks in 36.8° cones that contain a high muon multiplicity is approximately 9.5. In 13% of the cases, a cone containing two or more muons recoils against a similar cone. We are presently unable to explain this unexpected background through standard model processes in conjunction with our understanding of the CDF II detector, trigger and event reconstruction. We are continuing detailed studies with longer time for completion.

IX. ACKNOWLEDGMENTS

We thank the Fermilab staff and the technical staffs of the participating institutions for their vital contributions. This work was supported by the U.S. Department of Energy and National Science Foundation; the Italian Istituto Nazionale di Fisica Nucleare; the Ministry of Education, Culture, Sports, Science and Technology of Japan; the Natural Sciences and Engineering Research Council of Canada; the National Science Council of the Republic of China; the Swiss National Science Foundation; the A.P. Sloan Foundation; the Bundesministerium für Bildung und Forschung, Germany; the Korean Science and Engineering Foundation and the Korean Research Foundation; the Particle Physics and Astronomy Re-

search Council and the Royal Society, UK; the Institut National de Physique Nucleaire et Physique des Particules/CNRS; the Russian Foundation for Basic Research; the Comisión Interministerial de Ciencia y Tecnología, Spain; the European Community's Human Potential Programme; the Slovak R&D Agency; and the Academy of Finland.

[1] M. L. Mangano, P. Nason, and G. Ridolfi, Nucl. Phys. **B373**, 295 (1992).

[2] F. Happacher *et al.,* Phys. Rev. D **73**, 014026 (2006); F. Happacher, *Status of the Observed and Predicted $b\bar{b}$ Cross Section at the Tevatron*, `www − conf.kek.jp/dis06/doc/WG5/hfl20 − happacher.ps`, to appear in the Proceedings of DIS 2006, Tsukuba, Japan.

[3] G. Apollinari *et al.,* Phys. Rev. D **72**, 072002 (2005).

[4] D. Acosta *et al.,* Phys. Rev. D **69**, 012002 (2004).

[5] W.-M. Yao *et al.,* J. Phys. G **33**, 1 (2006).

[6] T. Aaltonen *et al.,* Phys. Rev. D **77**, 072004 (2008).

[7] F. Abe *et al.,* Phys. Rev. D **55**, 2546 (1997).

[8] B. Abbott *et al.,* Phys. Lett. B **487**, 264 (2000).

[9] F. Abe *et al.,* Nucl. Instrum. Methods Phys. Res., Sect. A **271**, 387 (1988).

[10] R. Blair *et al.,* Fermilab Report No. FERMILAB-Pub-96/390-E (1996).

[11] C. S. Hill *et al.,* Nucl. Instrum. Methods Phys. Res., Sect. A **530**, 1 (2004).

[12] A. Sill *et al.,* Nucl. Instrum. Methods Phys. Res., Sect. A **447**, 1 (2000).

[13] T. Affolder *et al.,* Nucl. Instrum. Methods. Phys. Res., Sect. A **453**, 84 (2000).

[14] T. Affolder *et al.,* Nucl. Instrum. Methods Phys. Res., Sect. A **526**, 249 (2004).

[15] G. Ascoli *et al.,* Nucl. Instrum. Methods Phys. Res., Sect. A **268**, 33 (1988).

[16] J. Elias *et al.,* Nucl. Instrum. Methods. Phys. Res., Sect. A **441**, 366 (2000).

[17] D. Acosta *et al.,* Nucl. Instrum. Methods Phys. Res., Sect. A **461**, 540 (2001).

[18] R. Downing *et al.,* Nucl. Instrum. Methods Phys. Res., Sect. A **570**, 36 (2007).

[19] M. M. Block and R. N. Cahn, Rev. Mod. Phys. **57**, 563 (1985).

[20] S. Klimenko *et al.,* Fermilab Report No. FERMILAB-FN-0741 (2003).

[21] B. Ashmanskas *et al.,* Nucl. Instrum. Methods Phys. Res., Sect. A **518**, 532 (2004).

[22] G. Marchesini and B. R. Webber, Nucl. Phys. B **310**, 461 (1988); G. Marchesini *et al.,* Comput. Phys. Commun. **67**, 465 (1992).

[23] D. J. Lange, Nucl. Instrum. Meth. A **462**, 152 (2001). We use version V00-14-05 downloaded from `http : //www.slac.stanford.edu/BFROOT/dist/packages/EvtGen/`.

[24] R. Brun *et al.,* CERN Report No. CERN-DD-78-2-REV; R. Brun *et al.,* CERN Programming Library Long Write-up W5013 (1993).

[25] F. Abe *et al.,* Phys. Rev. D **50**, 2966 (1994); T. Affolder *et al.,* Phys. Rev. D **64**, 032002 (2001); D. Acosta *et al.,* Phys. Rev. D **72**, 032002 (2005).

[26] D. Acosta *et al.,* Phys. Rev. D **69**, 072004 (2004).

[27] T. Shears, "Charm and Beauty Production at the Tevatron", Proceedings of the Int. Europhys. Conf. on High Energy Phys., PoS (HEP2005), 072 (2005).

[28] F. Abe *et al.,* Phys. Rev. Lett. **64**, 157 (1990).